

Indian plate structural inheritance in the Himalayan foreland basin, Nepal

Michael J. Duvall¹  | John W. F. Waldron¹  | Laurent Godin²  | Yani Najman³  | Alex Copley⁴ 

¹Department of Earth and Atmospheric Sciences, University of Alberta, Edmonton, AB, Canada

²Department of Geological Sciences and Geological Engineering, Queen's University, Kingston, ON, Canada

³Lancaster Environment Centre, Lancaster University, Lancaster, UK

⁴Department of Earth Sciences, University of Cambridge, Cambridge, UK

Correspondence

John W. F. Waldron, Department of Earth and Atmospheric Sciences, University of Alberta, Edmonton, AB, Canada.
Email: john.waldron@ualberta.ca

Funding information

Participation by J.W.F.W. and L.G. was supported by National Sciences and Engineering Research Council of Canada Discovery Grants. This paper was written while Y.N. was a visiting scholar at University of Colorado, Boulder, supported by a Cooperative Institute for Research in Environmental Sciences Visiting Fellow Program funded by National Atmospheric and Oceanic Administration Agreement NA17OAR4320101.

Abstract

The Himalaya, the Earth's largest active orogen, produces a deep but relatively unexplored foreland basin by loading the Indian Plate. Newly available two-dimensional seismic data (ca. 5,180 line km) spanning 900 km of the Nepali lowlands allow mapping and interpretation of several regional subsurface markers in two-way-travel time and estimated depth. Isopach maps for the major intervals allow us to interpret the interplay between basement structure, flexure, and faulting within the Ganga Basin. The Indian continental lithosphere beneath the foreland basin contains basement ridges oriented at high angles to the thrust belt. These basement structural highs and intervening depressions, tens to hundreds of kilometres wide, influenced deposition of the Precambrian Vindhyan strata and overlying Paleozoic to Mesozoic successions. The overlying Miocene to Quaternary foreland basin shows along-strike thickness variations across the basement features. Because the foreland basin sediments were mainly deposited in an alluvial plain close to sea-level, accommodation, and therefore thickness, was predominantly controlled by subsidence of the Indian Plate, providing evidence that the basement features controlled foreland basin development. Subsidence varied in time and space during Neogene basin development. When combined with flexural modelling, these observations imply that the subsidence history of the basin was controlled by inherited lateral variations in the flexural rigidity of the Indian Plate, as it was translated northward beneath the Himalayan Orogen. Basement features continue to play a role in higher levels of the thrust belt, showing that basement features in a down-going plate may produce non-cylindrical structures throughout orogen development.

KEYWORDS

foreland basin, Himalaya, lithospheric flexure, structural inheritance

1 | INTRODUCTION

Foreland basins result from flexure of continental lithosphere under the gravitational load of an adjacent orogen. The Himalaya, the Earth's largest currently active collisional orogen, has produced a deep foreland basin on the Indian Plate, but the large-scale geometry and evolution of the Himalayan foreland basin are relatively unexplored. In this paper, we use newly available seismic reflection data to describe the geometry of the Himalayan foreland basin in Nepal, and show that the subsidence of the basin has varied, both in time and in space, since the early Neogene. We suggest that these variations can be explained by lateral variations in the rigidity of the Indian Plate due to basement ridges that enter the orogen at a high angle to its regional trend, and test this hypothesis using a simple flexural model. Our results suggest that structures in the Indian Plate have had, and continue to have, profound effects on the development of the Himalaya and its foreland basins, and that basement structures at high angles to orogenic belts may have a similar influence in other orogens.

The Himalayan Orogen is the product of the ongoing continent-continent collision between the Indian and Eurasian plates that initiated in the Paleogene (Bouilhol et al., 2013; Hu et al., 2016; Najman et al., 2017). The Ganga Foreland Basin lies south of the Himalayan orogen and stretches east-west along the length of the orogen from Pakistan through India to Nepal (Figure 1) (Burbank et al., 1996; Lyon-Caen & Molnar, 1985). The present-day basin is occupied by the floodplain of the Ganges River. Underlying foreland-basin strata consist of fluvial deposits going back at least to the Miocene, unconformably underlain by Cretaceous to Paleogene marine strata. The apparent longitudinal continuity of the Ganga Basin sediments contrasts with along-strike differences (summarized by Godin et al., 2019) in Himalayan topography (Duncan et al., 2003), incision patterns (van der Beek et al., 2016), crustal density (Basuyau et al., 2013), structure (Yin, 2006), rates of convergence and exhumation (Burgess et al., 2012; McQuarrie et al., 2014), seismicity (de la Torre et al., 2007; Gahalaut & Kundu, 2012; Monsalve et al., 2006), and climate (Anders et al., 2006; Vögeli et al., 2017). Lithosphere-scale transverse basement faults in the Indian plate have potentially played a role in the segmentation of both the orogen and the Ganga Basin (Bollinger et al., 2004; Godin & Harris, 2014; Godin et al., 2019).

In the sections that follow, we first summarize the geological context of the Ganga foreland basin that extends ca. 900 km parallel to the strike of the orogen. We then interpret newly available 2D seismic reflection data from petroleum exploration in the Nepali segment of the basin, showing that stratigraphic thicknesses varied both in time and space. Our study then compares variations in thickness and basin

Highlights

- Seismic reflection data reveal the structure of the Himalayan foreland basin on the Indian Plate.
- Sediment thickness variations reveal changes in Cenozoic accommodation rate in both space and time.
- Indian Plate flexure beneath the Himalayan load was controlled by fault-bounded basement ridges.

geometry with the spatial distribution of subsurface ridges and associated deep-seated crustal faults in the Indian Plate below the basin. Using a flexural model for the Indian plate, we show that these basement features have played a major role in the subsidence history of the Ganga Basin.

2 | TECTONIC SETTING

2.1 | Himalayan Orogen: Major subdivisions

Four lithotectonic Himalayan domains (e.g. Avouac, 2003; Heim & Gansser, 1939) are bounded by a series of broadly north-dipping, but folded, continental-scale faults (Figure 1) most of which root into a geophysically imaged, gently dipping regional décollement, the Main Himalayan Thrust (MHT; Brown et al., 1996; Hauck et al., 1998; Nelson et al., 1996; Zhao et al., 1993). The northernmost lithotectonic domain is the Tethyan Himalaya, interpreted to have been deposited on the northern paleocontinental margin of India. The Tethyan Himalaya is bounded to the north by the Indus-Yarlung Zangbo Suture Zone (IYZS), and to the south by the South Tibet Detachment system (STD; Figure 1; Burchfiel et al., 1992; Kellett et al., 2019; Ratschbacher et al., 1994). Plutonic and high-grade metamorphic rocks of the Greater Himalaya occur between the STD and the Main Central Thrust (MCT; Heim & Gansser, 1939; Searle et al., 2008). Lower grade metasedimentary and metavolcanic rocks of the Lesser Himalaya, including foreland basin strata that are now allochthonous, are bounded (Figure 1) by the MCT and the Main Boundary Thrust (MBT; Gansser, 1964; DeCelles et al., 2020; MBT; Heim & Gansser, 1939). Finally, Cenozoic sedimentary rocks of the Sub-Himalaya, also transported, lie between the MBT and the active Main Frontal Thrust (MFT); these rocks represent exhumed foreland basin units, deposited during the rise of the Himalaya (Burbank et al., 1996). Foreland basin sediments and sedimentary rocks south of the MFT underlie the Indo-Gangetic Plain, extending ca. 400 to 450 km south of the MFT. Like the Sub-Himalayan

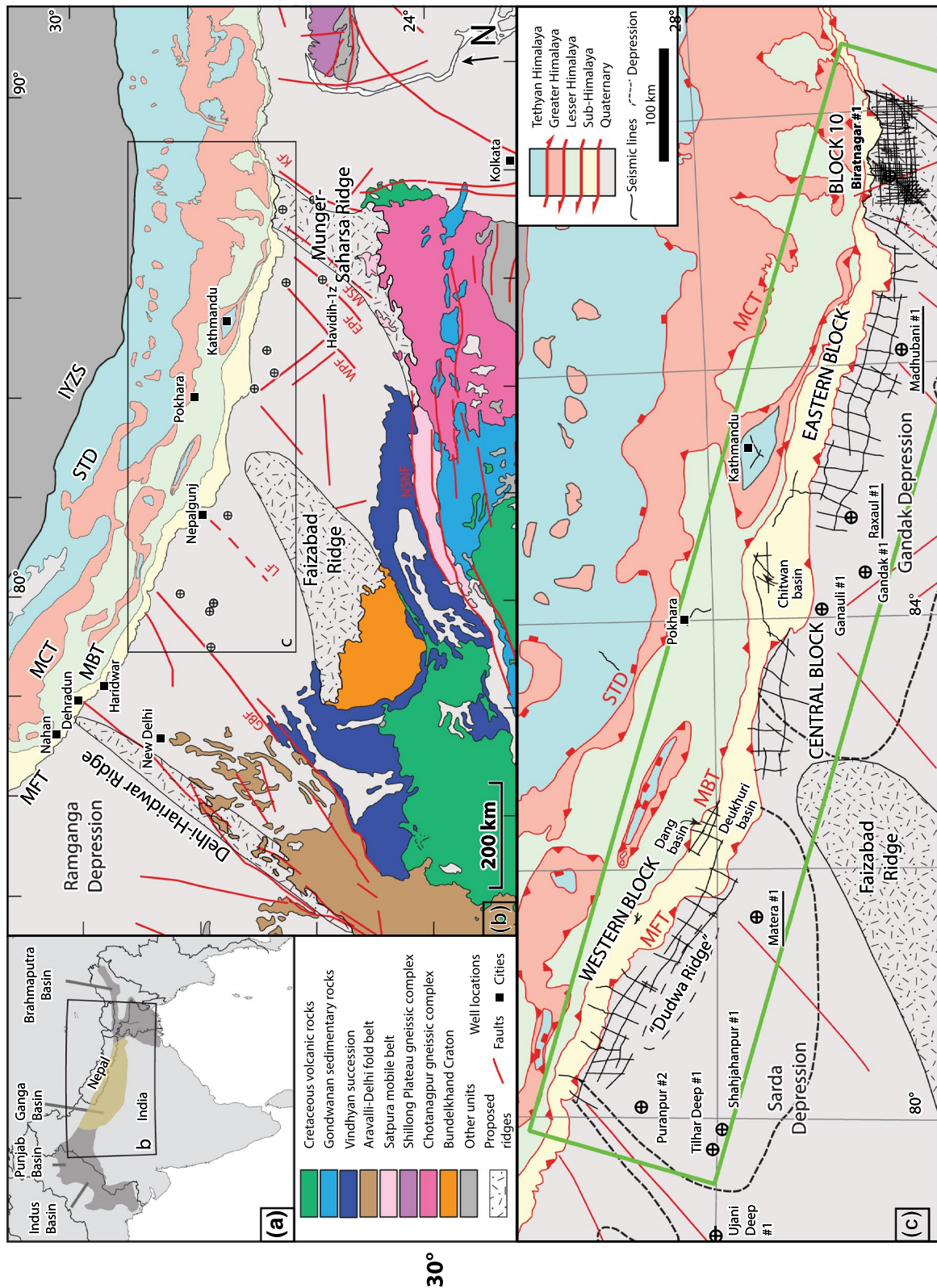


FIGURE 1 Regional maps. (a) Regional political map of south central Asia and major sedimentary basins underneath the Ganga Alluvial Plain; Ganga Basin highlighted after Rao (1973). (b) Generalized geology map of Northern India, Nepal, and adjacent areas after Casshyap and Khan (2000), Goscombe et al. (2018), Kellett and Grujic (2012), Mohanty (2012), Soucy la Roche et al. (2018) and Yin (2006), and United States Geological Survey public data. Approximate traces of basement ridges after Godin and Harris (2014). IYZS: Indus–Yarlung Zangbo Suture Zone; STD: South Tibet Detachment system; MCT: Main Central Thrust; MBT: Main Boundary Thrust; MFT: Main Frontal Thrust; KF: Kishangang Fault; MSF Munger-Saharsa Ridge Fault, WPF West Patna Fault; EPF: East Patna Fault; LF: Lucknow Fault; GBF: Great Boundary Fault; NSNF: North Son-Narmada Fault. (c) Detailed map of seismic lines and wells within the study area (location shown in b). Seismic surveys used in this study are highlighted. Green rectangle outlines area shown in location maps (Figures 5, 6 and 9)

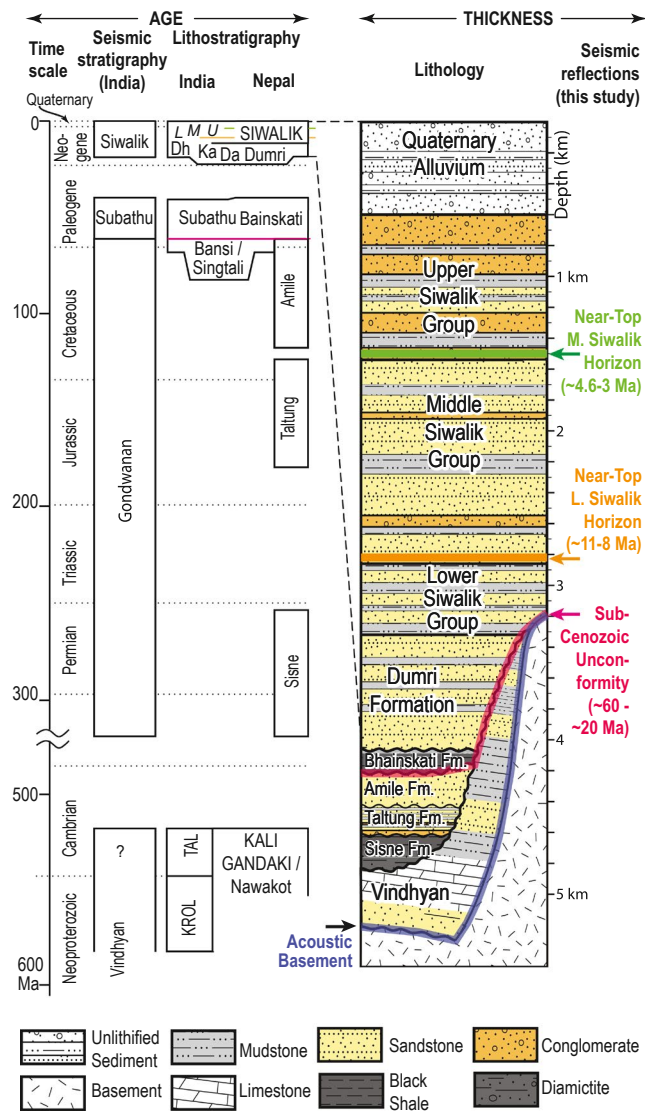


FIGURE 2 Generalized lithostratigraphic chart of the Ganga Basin and Sub-Himalaya, showing stratigraphic succession plotted against geologic age (left) and thickness (right). Group names shown as uppercase text. Timescale after Cohen et al. (2013). Seismic stratigraphy column after Srinivasan and Khar (1996). Lithostratigraphy of the Sub- and Lesser Himalaya of India after Hughes et al. (2005), Mathur (1978), Najman et al. (1997), Valdiya (1980), White et al. (2002). Lithostratigraphy of the Sub- and Lesser Himalaya of Western Nepal based on Najman et al. (2005), Ojha et al. (2009), Sakai (1983) and Upreti (1999). Alluvium and Siwalik Group thicknesses represent those in the Biratnagar-1 well; outcrop thicknesses from Sakai (1983) were used for older strata. Da - Dharamasala Formation; Ka - Kasauli Formation; Da - Dagshai Formation; L - Lower; M - Middle; U - Upper

sedimentary rocks, the foreland basin strata comprise sediment mainly derived from the erosional unroofing of the orogen, together with some input from the Indian continent to the south (Gansser, 1964). Accommodation space for these sediments is interpreted to have resulted from flexural

subsidence driven by the weight of the Himalaya (DeCelles et al., 1998; Lyon-Caen & Molnar, 1985).

2.2 | Basement structure

The Cenozoic sedimentary rocks of the Himalayan foreland basin were deposited on a succession of Late Carboniferous to Cretaceous sedimentary strata derived from the margin of Gondwana (the Gondwana succession), underlain by Proterozoic stratified rocks of the intracratonic Vindhyan basin, in turn underlain by older, more deformed basement units (Gansser, 1964; Krishnan, 1949; Rasmussen et al., 2002; Ray, 2006; Ray et al., 2002; Veevers & Tewari, 1995) (Figure 2). At its southern boundary (Figure 1b), the Ganga Basin (Rao, 1973) oversteps multiple Archean and Proterozoic basement provinces and mobile belts (Balakrishnan et al., 2009; Mitra et al., 2011; Sastri et al., 1971; Valdiya, 1976). From west to east, the basin onlaps the Proterozoic Aravalli-Delhi fold belt (Sastri et al., 1971; Valdiya, 1976), the Vindhyan succession in the Sarada depression, the Bundelkhand Craton, primarily Archean granite (Sharma & Rahman, 2000), the Proterozoic Vindhyan succession (Meert et al., 2010) in the Gandak depression, the Proterozoic Satpura Mobile Belt (Meert et al., 2010; Mohanty, 2012), and the ca. 2,300 to 1,000 Ma Chotanagpur Gneissic Complex (Chatterjee & Ghose, 2011; Mohanty, 2012) (Figure 1b). Significant variations in crustal seismic velocity ratios are seen along-strike (Mitra et al., 2011), reflecting changes from granitic to mafic and sedimentary compositions as the foreland basin oversteps these units.

Through correlations between surficial mapping, gravity and magnetic anomaly studies, and rare boreholes, regional NE-SW basement highs or ‘spurs’ have been interpreted under the Ganga foreland basin (Godin & Harris, 2014; Karunakaran & Rao, 1979; Raiverman et al., 1994; Rao, 1973; Sengupta, 1962; Shukla & Chakraborty, 1994; Valdiya, 1976). These ridge systems have been invoked to explain the spatial distribution and thickness variation of Gondwanan and Cenozoic successions (Raiverman, 1983; Raiverman et al., 1994; Rao, 1973). Recent structural and geophysical work suggests that associated deep crustal faults may have been reactivated through time (Godin & Harris, 2014; Godin et al., 2019; Soucy La Roche & Godin, 2019).

Three of these ridges are portrayed in Figure 1. The *Delhi-Haridwar* ridge is a ca. 50 km wide horst containing the Proterozoic Aravalli mobile belt; the *Faizabad* ridge correlates with the granite and gneiss-dominated Bundelkhand Craton; and the *Munger-Saharsa* ridge includes the sub-surface expression of the Satpura mobile belt (Figure 1) (Valdiya, 1976). Numerous smaller basement highs or ‘spurs’ correspond to crustal-scale lineaments, mainly in the western

portion of the Ganga Basin (Raiverman, 1983; Raiverman et al., 1994). The Gandak and Sarda Depressions (Figure 1c) occur east and west of the Faizabad ridge, respectively, and accommodate significant deposits of Proterozoic and Paleozoic sedimentary strata (Raiverman, 1983; Raiverman et al., 1994; Sastri et al., 1971). Raiverman (1983, 2002) interpreted a small basement high trending E-W within the Sarda depression, termed the Dudwa ridge (Figure 1c).

Crustal-scale faults, also at high angles to the Himalayan Orogen, have been identified under the Ganga Basin, including (from east to west) the Kishangang basement fault, the Munger-Saharsa Ridge fault, the West and East Patna faults, the Lucknow fault, and the Great Boundary fault (Figure 1b) (Aditya et al., 1979; Dasgupta, 1993; Dasgupta et al., 2013; Godin & Harris, 2014; Karunakaran & Rao, 1979; Raiverman et al., 1994; Rao, 1973; Sastri et al., 1971). These faults are deep-seated, and typically show normal offsets below the foreland basin strata, without disrupting Cenozoic foreland strata (Raiverman et al., 1994). Many of these faults coincide with the edges of NE-SW basement ridges (Godin & Harris, 2014; Godin et al., 2019). These ridge/fault systems are interpreted as horsts (Godin & Harris, 2014; Godin et al., 2019), and their reactivation may have influenced along-strike sediment distributions in the Ganga Basin (Raiverman, 1983; Raiverman et al., 1994).

Faults at the scale of seismic reflection profiles have been described in the Nahan-Dehradun-Haridwar area (Figure 1b) where they are grouped into two trends: a predominantly NW-SE population of normal faults parallel to the Himalayan Orogen, and a N-S set interpreted as predominantly dextral (Raiverman et al., 1994). Both sets only cut pre-Cenozoic strata in the foreland basin, suggesting movement is pre-Cenozoic. However, within the thrust belt, the N-S population cuts Miocene strata; Raiverman et al. (1994) interpreted this difference of fault timing to indicate fault reactivation in the thrust belt.

2.3 | Stratigraphy of the Ganga foreland basin

The stratigraphy of the Ganga foreland basin is best known from exposures in thrust sheets of the Sub-Himalaya and Lesser Himalaya. South of the MFT the subhorizontal stratigraphy has been largely defined by a series of wells in India (Fuloria, 1996; Karunakaran & Rao, 1979; Sastri et al., 1971; Srinivasan & Khar, 1996) and a single well in Nepal (Biratnagar-1; Figure 1c), which did not penetrate the basement. In this paper, we use the Nepalese stratigraphy, although formation names vary along strike (Figure 2). Four subsurface sedimentary successions or megasequences have been recognized. From base to top, the successions are: (a) the Vindhyan succession of the intracratonic Vindhyan Basin, interpreted by some authors (e.g. Srinivasan & Khar, 1996) as

extending into the early Cambrian but regarded by others (e.g. Meert & Pandit, 2015) as entirely Proterozoic; (b) the Late Carboniferous/Permian to Cretaceous Gondwanan succession, deposited on the northern margin of continental India; (c) the Paleocene to Eocene Bhainskati Formation (Subathu sequence in India; Srinivasan & Khar, 1996), representing the earliest Himalayan foreland basin deposits; and (4) the Neogene to Quaternary Dumri–Siwalik succession (DeCelles et al., 1998). A comparison between stratigraphic columns plotted against time and distance (Figure 2) underscores an increased sedimentation rate by over two orders of magnitude during the Neogene and Quaternary, compared with the previous history of the margin, recording both rapid flexural subsidence of the Indian lithosphere and abundant sediment supply from the Himalaya.

2.3.1 | Vindhyan succession

South of the Ganga Plain, the Bundelkhand craton is flanked by the intracratonic Vindhyan basin, bounded to the west by the Aravalli Mountains, and to the southeast by the North Son–Narmada Fault (Shukla & Chakraborty, 1994). The basin contains (Figures 1b and 2) relatively undeformed and unmetamorphosed Proterozoic sandstone, mudstone, and carbonate, with subordinate conglomerate and volcanoclastic horizons (Bhattacharyya, 1996; Bose et al., 2015; Meert et al., 2010). A regional unconformity divides this Vindhyan succession into upper and lower units (Ray, 2006).

The Vindhyan succession has been intersected by deep exploration wells in India (Shukla & Chakraborty, 1994), where some authors have distinguished it as the Ganga Supergroup (Fuloria, 1996; Prasad & Asher, 2001). We use the same term, Vindhyan succession, for both the exposed and subsurface units. The succession was preferentially deposited between the main basement ridges (Karunakaran & Rao, 1979; Negi & Eremenko, 1968), suggesting that Proterozoic movement of the bounding faults accommodated and localized Vindhyan strata (Gahalaut & Kundu, 2012; Godin & Harris, 2014; Raiverman et al., 1994). An angular unconformity separates the Vindhyan succession from overlying units (Rao, 1973).

2.3.2 | Gondwanan succession

Gondwanan (Late Carboniferous/Permian to earliest Paleogene) strata on the Indian subcontinent are largely restricted to basins coinciding with suture zones between Archean cratons, and show graben or half-graben geometries (Biswas, 1999; Mukhopadhyay et al., 2010; Veevers & Tewari, 1995). These strata have been interpreted

(Sakai, 1983) as representing the northern Indian continental margin (DeCelles et al., 2004; Sitaula, 2009), initiated as rift basins associated with Gondwana breakup (Biswas, 1999). However, the source of the Gondwanan succession has been interpreted as the Bhimphedian Orogen, which lay along the north margin of Gondwana (Cawood et al., 2007; Grujic et al., 2017).

In the Lesser Himalaya of Nepal, Gondwanan strata have a broad spatial distribution (Sakai, 1983; Sitaula, 2009). In the Ganga Basin subsurface, their presence is more doubtful. Gondwanan strata may be preserved in the area covered by the seismic data interpreted here (Bashyal, 1998; Fuloria, 1996). However, Mesozoic strata previously reported (Sastri et al., 1971) in the Tilhar-1, Ujani-1 and Puranpur-2 wells (Figure 1c) have been reinterpreted as Proterozoic to possibly Cambrian (McKenzie et al., 2011; Xiao et al., 2016).

2.3.3 | Paleogene Bhainskati Formation – Early foreland basin deposits

The Bhainskati Formation (Figure 2), >90 m thick in outcrop in the Lesser Himalaya, overlies Gondwanan deposits that predate Himalayan orogenesis (DeCelles et al., 1998; Sakai, 1983). The basal contact is concordant in outcrop (Sakai, 1989; Sakai et al., 1992), marking an upward transition from quartzose sandstone of the Amile Formation to fossiliferous organic-rich shale, with infrequent sandstone and oolitic ironstone, characteristic of a shallow marine environment (DeCelles et al., 2004; Sakai, 1983). The contact is interpreted to be at least as young as 60 ± 8 Ma (Najman et al., 2005), and signifies a shift from peninsular Indian provenance to the combined Himalaya and Indian sources (DeCelles et al., 2004; Garzanti, 2019; Ravikant et al., 2011). The uppermost Bhainskati Formation is lateritic paleosol, interpreted as a residual deposit below an unconformity (DeCelles et al., 1998) constrained as <45 Ma (Najman et al., 2005). The Bhainskati Formation is interpreted as representing deposition in the back-bulge portion of the early Ganga foreland basin (DeCelles et al., 2004), although the existence of this back-bulge is disputed (Garzanti, 2019).

2.3.4 | Neogene to Quaternary: Dumri Formation and Siwalik Group

The clastic Dumri Formation (and equivalents in India; Figure 2) is of variable exposed thickness; the true thickness is difficult to determine as the unit is typically fault-bounded. For example, the unit is >700 m thick at its type section in Central Nepal where the top is not exposed, and >1,200 m

thick at Swat Khola in western Nepal, where the top is thrust-truncated (DeCelles et al., 1998; Sakai, 1989). The regional unconformity at its base is interpreted variously as a product of: a peripheral bulge related to the advancing load of the Himalaya (DeCelles et al., 1998), a redistribution of that load (Najman et al., 2004); or of mantle processes such as slab break-off (Garzanti, 2019; Najman et al., 2018). The Dumri Formation is dominated by trough cross-stratified and planar sandstone beds that represent channel fills, crevasse splays, and paleosols (DeCelles et al., 1998). Its maximum depositional age from detrital zircon fission track analysis is 28–24 Ma (Najman et al., 2005; Stickroth et al., 2019), but it is constrained by magnetostratigraphy between ca. 19.9 and 15.1 Ma in western Nepal (Ojha et al., 2009), suggesting a long hiatus between the Bhainskati and Dumri Formations. The Bhainskati and Dumri Formations are restricted to the Lesser Himalaya of Nepal, although equivalents occur in the Sub-Himalaya in India and in deeper parts of the Ganga basin (Fuloria, 1996; Raiverman et al., 1994).

The Siwalik Group (Figures 2 and 3) is the thickest accumulation of Himalaya-derived detritus in the Ganga Basin (DeCelles et al., 1998, 2020; Sahni & Mathur, 1964). It consists of fluvial mudstone, sandstone, and conglomerate, with a similar depositional style to the modern Indo-Gangetic plains (Parkash et al., 1980). An informal tripartite division into the lower, middle, and upper Siwalik Group was first based on vertebrate markers (Pilgrim, 1913), but later refined to reflect lithological contrasts between mudstone-, sandstone- and conglomerate-dominated facies, respectively (Karunakaran & Rao, 1979; Sahni & Mathur, 1964). Although the Siwalik Group has been further subdivided into formations in some areas (e.g. Corvinus & Rimal, 2001; Dhital, 2015; Kumar & Tandon, 1985; Nakayama & Ulak, 1999), the tripartite division is used in this study. A magnetostratigraphic boundary constrains its base to >ca. 15.5 Ma in Nepal (Gautam & Fujiwara, 2000). Other magnetostratigraphic studies in Nepal have placed the lower to middle Siwalik contact between 11.05 and 8.0 Ma, and the middle to upper Siwalik contact between 4.6 and 3.0 Ma (Ojha et al., 2000, 2009; Rösler et al., 1997). However, magnetostratigraphic correlation also suggests that these boundaries are diachronous, spanning ca. 2 Ma (Ojha et al., 2009). The overall coarsening-upward trend has been attributed to cratonward migration of the thrust front through time (DeCelles et al., 1998, 2020).

The lower Siwalik Group (middle Miocene) reaches thicknesses ca. 1,400 m and consists of fluvial and paleosol deposits (DeCelles et al., 1998; Mugnier et al., 1999; Quade et al., 1995). Sandstone lenses are typically 2–5 m thick and intercalated with bedded floodplain deposits on a scale of <1 to 10 m (Quade et al., 1995). The middle Siwalik Group (upper Miocene to Pliocene; Figure 2) is dominated by thick sandstone beds punctuated by thin siltstone and minor conglomerate horizons, deposited in fluvial/floodplain environments (Bernet et al., 2006; Quade et al., 1995). Channelfills



FIGURE 3 Field photographs. (a) Contact between the middle and upper Siwalik Group as observed in the Sub-Himalaya near Nepalgunj, geologist for scale: 1.78 m. (b) View of the contact between the lower and middle Siwalik Group, north of Nepalgunj, in the Sub-Himalaya. Topographic relief visible on the far ridgeline is approximately 300 m

are up to 20 m thick. The Pliocene to Quaternary upper Siwalik Group contains abundant conglomerate, together with sandstone and siltstone beds, diagnostic of proximal fluvial, braided stream, or alluvial fan deposits (Kumar & Tandon, 1985). Exposed sections in the Sub-Himalaya are ca. 2,100 m thick (e.g. Quade et al., 1995). The contact between the middle and upper Siwalik Group is typically defined based on the first major (>1 m) influx of conglomerate (Figure 3). Locally the contact is marked by either a disconformity or an angular unconformity (Mugnier et al., 1999), suggesting that parts of the upper Siwalik Group within the sub-Himalaya were deposited in piggy-back basins upon developing thrust sheets. A poorly defined but closely similar unit of “Quaternary alluvium” is recognized in some studies (e.g. Hartsink & Pradhan, 1989), but we have not attempted to separate this from the upper Siwalik Group. The upper Siwalik succession is estimated at ca. 1,105 m thick in the Sub-Himalaya (Mugnier et al., 1999), but exposed sections are truncated either by thrusts or by the present-day erosion surface.

2.4 | Structure in the foreland basin sedimentary rocks

The Siwalik Group in the Sub-Himalaya (north of the MFT) forms a classic thrust belt, dominated by a series of north-dipping thrusts that have folded and displaced strata southward (Mugnier et al., 1999) as the Himalayan tectonic wedge propagated into the foreland basin. Fault-propagation folds

(blind and emergent), duplexes, open folds, north-dipping monoclines, and south-dipping backthrusts have all been documented within the Sub-Himalaya (Almeida et al., 2018; Hirschmiller et al., 2014; Husson & Mugnier, 2003; Mugnier et al., 1999). Small intermontane basins exist within the thrust belt, including the Deukhuri, Dang, and Chitwan basins (Figure 1c). Central parts of the Sub-Himalaya are characterized by large-offset reverse faults and intervening open folds. Towards the MBT, at the north edge of the Sub-Himalaya, imbricated horses are documented (Mugnier et al., 1999).

In southeastern Nepal (Block 10 in Figure 1c) a series of approximately N-S tear faults that offset the foreland basin strata have recently been identified (Duvall et al., 2020). Although these are located over the Munger-Saharsa basement ridge, the basement faults associated with the ridge have a distinctly different strike. The N-S faults are interpreted as tear faults detached above a blind Outer Frontal Thrust that has propagated ca. 37 km south of the MFT since ca. 0.5 Ma (Duvall et al., 2020). At the leading southern edge of this structure, an incipient tectonic wedge is responsible for the uplift of the Bhadrapur High, a topographic feature that rises ca. 60 m above the surrounding Ganga plain. These structures provide a snapshot of early stages in the development of structures similar to those exposed in the Sub-Himalaya.

3 | DATA AND METHODS

The geometry of the Ganga Basin is here assessed through interpretation of 181 seismic profiles that span the Himalayan

foothills in Nepal (Figure 1c). Four blocks of data were made available, termed the 'Western Block', 'Central Block', 'Eastern Block', and 'Block 10' (Figure 1c). Further details are provided in the supporting information.

Only a single well is located within the 2D seismic grid: Biratnagar-1 (Figure 1c). This vertical well intersected two regional boundaries (Figures 4–6) but was abandoned before reaching its target depth. The contact at the top of the middle Siwalik Group is expressed as a 3 m interval of 'limey dolomite' (possibly a caliche or lacustrine unit) capping the sandstone and mudstone interbeds characteristic of the unit (Hartsink & Pradhan, 1989). Overlying strata include abundant conglomerate. The top of the lower Siwalik Group is marked by a >50 m sandstone interval overlying interbedded mudstone and sandstone. The basal 207 m of the well penetrated interbedded sandstone and mudstone, initially interpreted to be Gondwanan or Vindhyan rocks (Hartsink & Pradhan, 1989), but palynological data analyzed after the initial well report constrained their age to late Eocene or younger; several palynomorphs were reported to be more diagnostic of Miocene age, consistent with the Dumri Formation (Hartsink & Pradhan, 1989: Addendum), the interpretation adopted here. Because neither Gondwanan nor Vindhyan strata were penetrated, we have not distinguished between these two successions in our interpretations of seismic data.

Seismic data were depth-converted using a simple relationship based on checkshot data from Biratnagar-1 and two wells in adjacent India (Figure 4; see supplementary information for details). Because of uncertainties in the velocities, estimated depths may differ from true depths by $\pm 10\%$. However, because of the relative uniformity of the Siwalik Group lithologies throughout Nepal, such errors are likely to apply across the entire data set, and are therefore unlikely to affect our major conclusions on relative thickness changes.

Four regional reflectors are here mapped (Figure 7) across the 900 km-wide study area: the top of the acoustic basement (also referred to as the 'blue horizon'), a widespread unconformity at the base of the inferred Cenozoic succession (the sub-Cenozoic unconformity or 'pink horizon'), a horizon near the top of the lower Siwalik Group ('orange' horizon), and a horizon near the top middle Siwalik Group ('green' horizon). Wells in adjacent India (Madhubani-1, Raxaul-1 and Matera-1) were drilled within 9, 2, and 29 km, respectively, of the seismic grid (Figure 1c). Data from these wells were projected down-dip onto the closest seismic lines as an independent check on the consistency of our horizon picks across southern Nepal. Regional dip angles may be estimated using the contours (Figure 7) on these maps. Stratigraphic thicknesses were calculated from the depth-converted structural surfaces, and converted into isopach maps (Figure 8).

To supplement the seismic and well data, we examined key outcrop sections described previously in the fold-thrust belt of Central Nepal (Appel et al., 1991; DeCelles et al., 1998;

Mugnier et al., 1999; Ojha et al., 2009; Quade et al., 1995; Regumi et al., 2011; Rösler et al., 1997; Szulc et al., 2006). Two of the main seismic reflectors (the tops of the lower and middle Siwalik Group) correspond to lithostratigraphic boundaries that form prominent topographic lineaments, showing lateral continuity from mountainside to map scale (Figure 3). Although the resolution of the seismic data (see supporting information) did not warrant a detailed seismic facies analysis, the seismic character of the three interpreted Siwalik divisions matched well with the outcrop and lateral continuity characteristics of facies the corresponding units in outcrop. For example, reflection continuity was poor in the upper section, interpreted as mainly upper Siwalik channelized conglomerates, and was moderate to good in the interpreted lower Siwalik succession, in which laterally extensive floodplain deposits occur in outcrop.

To examine the underlying cause of the Cenozoic sediment thickness variations, we considered the controls on the flexure of the Indian plate as it is thrust beneath the Himalaya and Tibetan Plateau. When the lithosphere is flexed by a load, the across-strike wavelength of the displacements is controlled by the elastic thickness, and the amplitude of the displacements by both the elastic thickness and the size of the imposed load (e.g. Turcotte & Schubert, 2014). The long-wavelength elevation of the Tibetan Plateau is relatively constant along strike, implying no major along-strike changes in the degree of loading of the foreland lithosphere that could account for the lateral variation in Cenozoic sediment thickness. We therefore constructed a model to investigate what degree of along-strike variation in elastic thickness could reproduce the observations, and then compared our results to the possible degree of lateral heterogeneity within the Indian plate.

4 | OBSERVATIONS AND RESULTS

4.1 | Faults

Faults and folds at seismic scale within the foreland-basin sedimentary package are relatively uncommon (Figure 5) except close to the trace of the MFT (Figure 6); consequently, most foreland-basin strata appear subhorizontal and undisturbed in longitudinal section (e.g. Figure 5 from 0 to 4 km). Interpreted faults in the seismic data coincide with areas of low signal coherence across which reflections are offset. Most shallow faults are only identified on single lines, but in a detailed study of closely spaced lines in Block 10, Duvall et al. (2020) identified steep faults (Figure 5d), interpreted as tear faults above the newly identified Outer Frontal Thrust (OFT; Figure 6d). Minor uplifts and subsided areas (Figure 5d) up to 5 km in diameter are located adjacent to restraining and releasing bends on the tear faults,

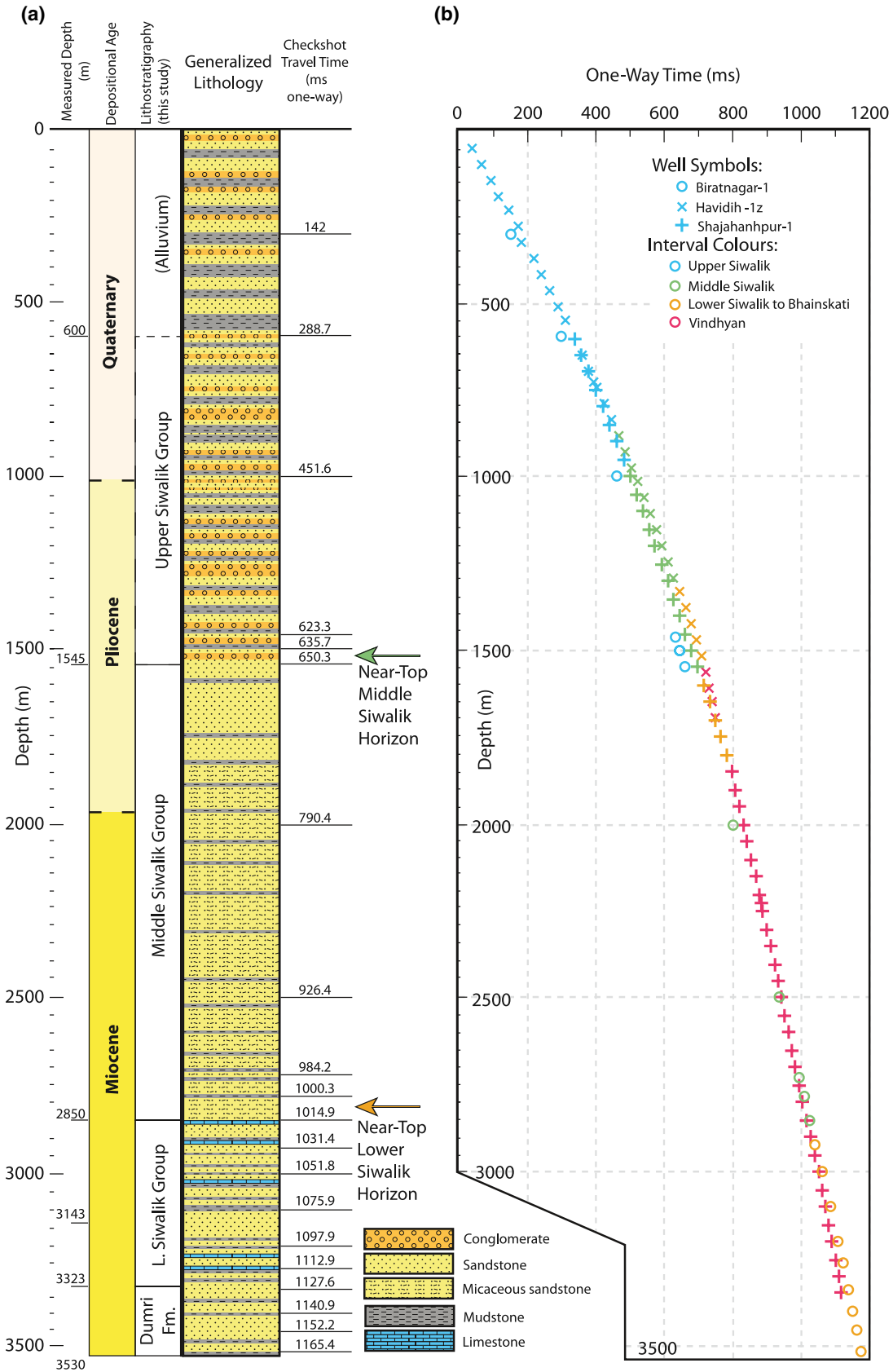


FIGURE 4 Well log and regional checkshot data. (a) Lithostratigraphic column representing strata intersected by the Biratnagar-1 well. Corresponding horizons picks are indicated in time. Neither the acoustic basement nor the sub-Cenozoic unconformity were intersected (Hartsink & Pradhan, 1989). (b) Checkshot data compiled from the Biratnagar-1, Havidih-1z, and Shajahanpur-1 wells, used for calculating a regional time-depth relationship. Well locations shown in Figure 1. Well tie to seismic data is shown in (d)



FIGURE 5 Representative depth-converted seismic profiles subparallel to the basin axis, illustrating well tie, seismic character of the foreland basin fill, faults and basement features. Inset map shows line locations in area outlined in Figure 1c. Faults in profile (d) as interpreted by Duvall et al. (2020). Uninterpreted versions are provided in the supplementary information

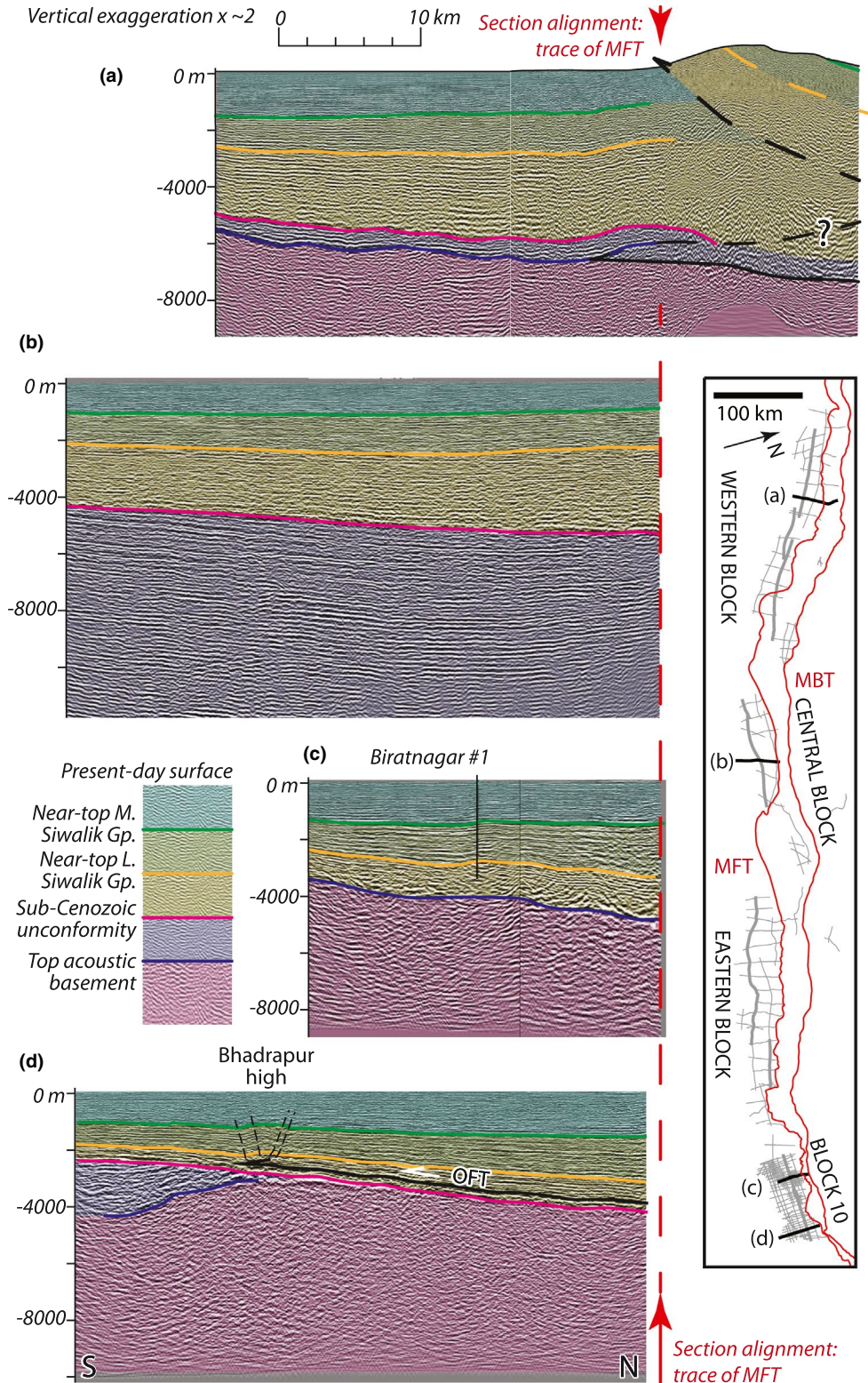


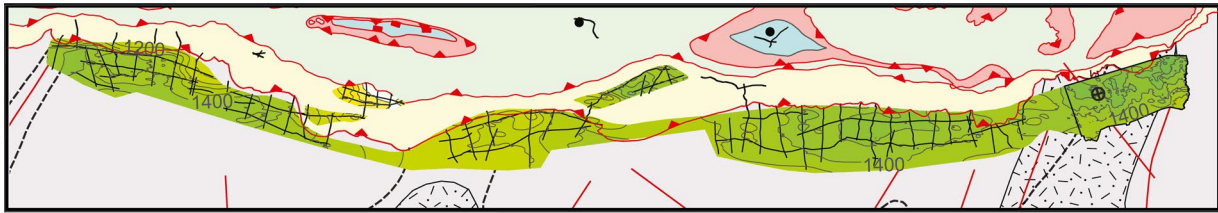
FIGURE 6 Representative depth-converted seismic profiles transverse to the basin axis, illustrating thickening toward the orogen in the foredeep, the positions of the Main Frontal Thrust and the Outer Frontal Thrust as interpreted by Duvall et al. (2020), and poorly resolved Sub-Himalayan structure. Inset map shows line locations in area outlined in Figure 1c. Faults in profile (d) as interpreted by Duvall et al. (2020). Uninterpreted versions are provided in the supplementary information

and a larger uplift, ca. 15 km wide, overlies the southern tip-line of the OFT beneath the Bhadrapur topographic high (Figure 6d). Despite their significance for modern

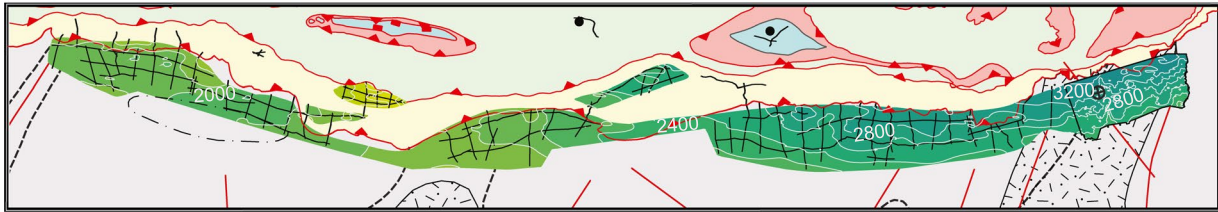
seismicity, these fault-related features have only localized impact on the regional patterns of structure and thickness in the Siwalik Group.

(a) Near-top middle Siwalik Group

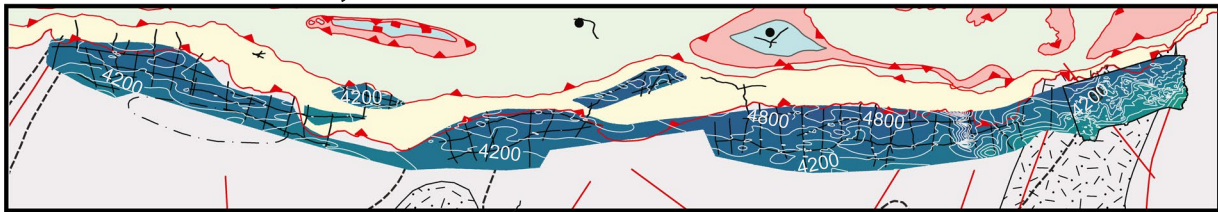
Elevation (m)



(b) Near-top lower Siwalik Group



(c) Sub-Cenozoic unconformity



(d) Top acoustic basement

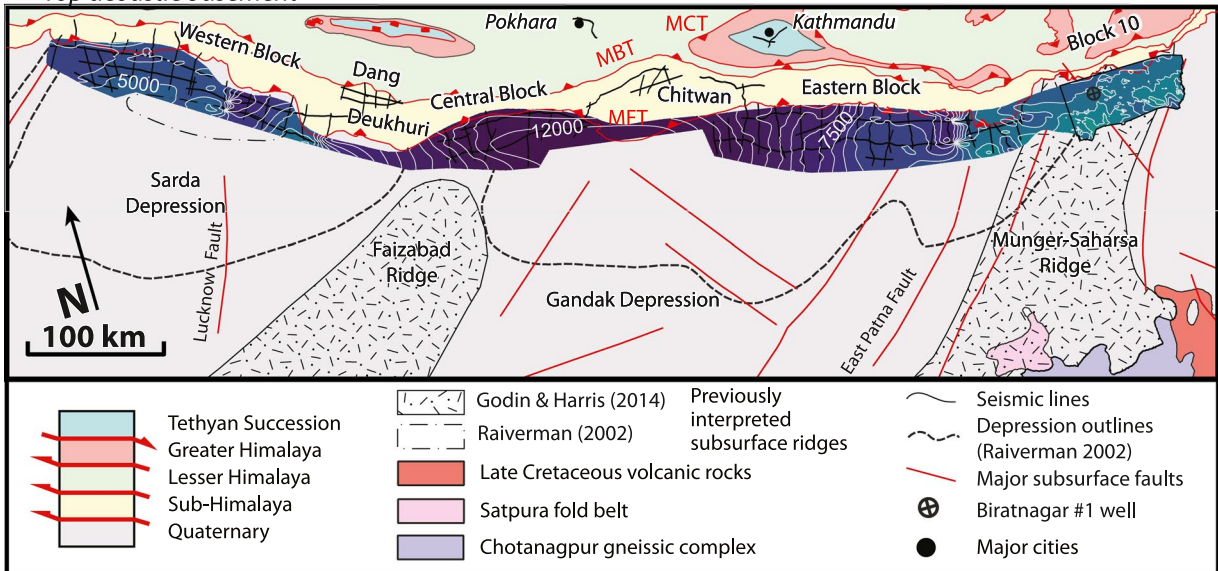


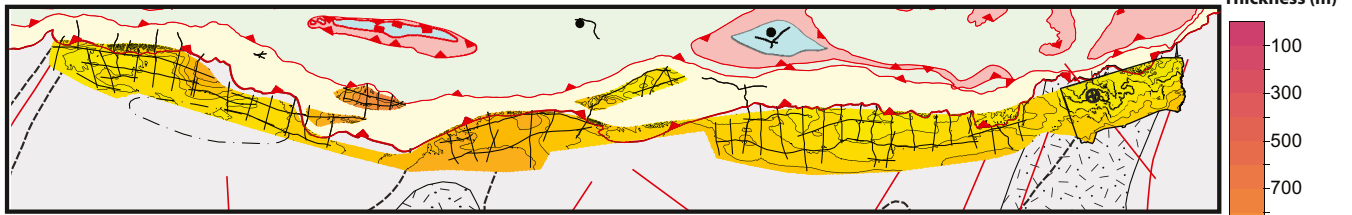
FIGURE 7 Structural maps of regional marker horizons. (a) Near-top middle Siwalik Group, contour interval 100 m. (b) Near-top lower Siwalik, contour interval 200 m (c) sub-Cenozoic unconformity, contour interval 200 m. (d) Acoustic basement, contour interval 500 m. Note that depths >12 km are unconstrained by data. Elevations are relative to sea level. Major structural features from Godin and Harris (2014) and Raiverman (2002). MCT: Main Central Thrust; MBT: Main Boundary Thrust; MFT: Main Frontal Thrust

Deeper in the section, below the sub-Cenozoic unconformity, steep faults with normal offsets (Figure 5a,c) bound graben and half-graben containing inferred Vindhyan to Gondwanan strata. These faults correspond, in general location and dip, with the basin-bounding faults interpreted by Godin and Harris (2014) on the basis of gravity data.

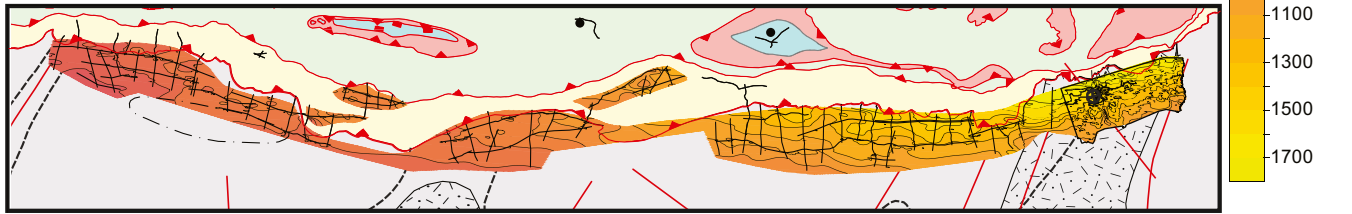
4.2 | Features of the structure maps

Figure 7 shows the structural elevation of the depth-converted horizons representing near-top middle Siwalik Group (green horizon; Figure 7a), near-top lower Siwalik Group (orange horizon; Figure 7b), sub-Cenozoic

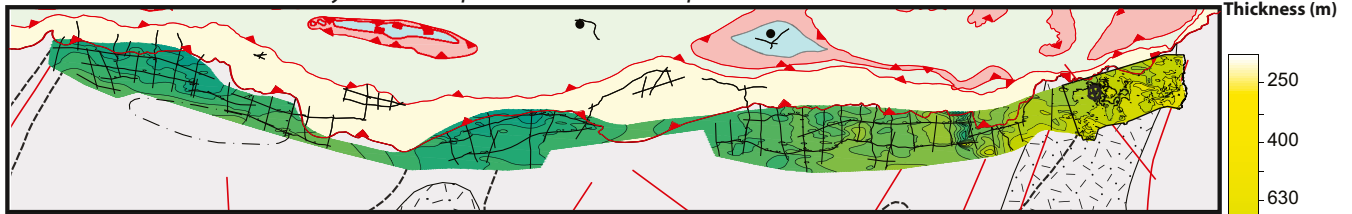
(a) Near-top middle Siwalik Group to DEM



(b) Near-top lower Siwalik to near-top middle Siwalik Group



(c) Sub-Cenozoic unconformity to near-top lower Siwalik Group



(d) Top acoustic basement to Sub-Cenozoic unconformity

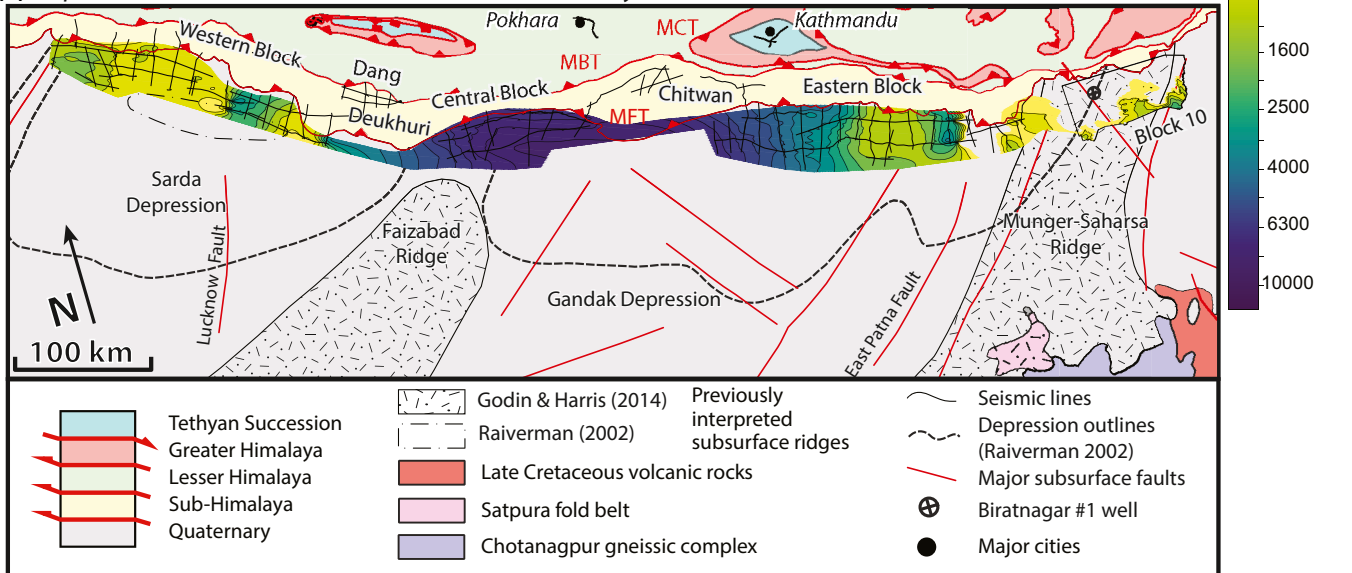


FIGURE 8 Isopach maps of regional marker horizons. (a) Surface to near-top middle Siwalik, contour interval 100 m. (b) Near-top middle Siwalik to near-top lower Siwalik, contour interval 100 m. (c) near-top lower Siwalik to sub-Cenozoic unconformity, contour interval 200 m. (d) Sub-Cenozoic unconformity to acoustic basement, contour interval 500 m. Major structural features from Godin and Harris (2014) and Raiverman (2002). MCT: Main Central Thrust; MBT: Main Boundary Thrust; MFT: Main Frontal Thrust

unconformity (pink horizon, Figure 7c), and acoustic basement (blue horizon; Figure 7d). Elevations are measured relative to sea-level; hence most elevation values on the traced horizons are negative.

4.2.1 | Top of acoustic basement (blue)

Figure 7d shows the elevation structure of the nonconformity (blue horizon) between igneous and metamorphic rocks of

the Indian basement and overlying stratified deposits. In far-eastern Nepal (Block 10), the Munger-Saharsa ridge is recognizable as a feature that peaks at $-3,000$ to $-4,000$ m. This regional high extends northwards to the MFT, and is locally cut by smaller-scale features (Figure 1c) interpreted as normal faults of ca. 275 to 950 m separation that may have been active during deposition of the Vindhyan to Gondwanan successions. The western edge of the ridge is marked by the East Patna Fault, interpreted as a normal fault with ca. 2,500 m dip separation (Figures 1c and 5c). Farther west, the basement gradually shallows, and then deepens into the Gandak depression (Figure 7d). The depression is characterized by seismic reflections extending to the maximum survey depth (6 s TWT), corresponding to depths of at least 12 km; hence the mapped elevations result from interpolation between the eastern and central blocks. Along the western margin of the Gandak basin, a gradational shallowing of the basement is observed towards the eastern flank of the Faizabad ridge. West of the inferred Faizabad ridge (where data are lacking), the acoustic basement is typically between $-6,200$ and $-6,700$ m, with local basement highs between $-5,000$ and $-5,100$ m in the eastern part of the Western Block, where the basement undulates to form a small trough from $-8,600$ to $-5,800$ m, suggesting a more complex topography than the Dudwa ridge interpreted in this region by Raiverman (2002). At the west end of the Western Block, the basement dips gently (ca. 2.5°) north at elevations of ca. $-5,500$ to $-6,500$ m. North of the MFT, acoustic basement depth is uninterpreted because of incoherency in the profiles probably due to subsurface deformation or data acquisition difficulties in rugged topography.

4.2.2 | Sub-Cenozoic unconformity (pink)

The sub-Cenozoic unconformity (pink horizon) shows more gradational changes in slope throughout, except in some parts of Block 10 where it coincides with the top of acoustic basement (Figure 7c). A northward-deepening trend (1.0° – 1.5° dip) continues north of the MFT beneath the Deukhuri, Dang, and Chitwan intermontane basins. However, in Block 10 and the Western Block, local northward shallowing within ca. 10 km of the surface trace of the MFT is interpreted to result from deformation close to the MFT (Figure 6a). A prominent structural high correlating with the Munger-Saharsa ridge occurs in Block 10, where the elevation of the unconformity ranges between $-2,800$ and $-4,000$ m, with northward dips of ca. 2.5° . The unconformity is at its deepest in a wide basin in the Eastern and Central Blocks, corresponding to the Gandak depression, where elevations range from $-4,700$ to $-5,700$ m. To the west, a shallowing of the sub-Cenozoic unconformity corresponds to the interpreted location of the Faizabad Ridge. Two discrete depressions, reaching depths $-5,500$

to $-5,800$ m, occupy the Western Block: a small structural high exists in the southwest extremity of this block, to the west of, and in contrast to the inferred Dudwa ridge of Raiverman (2002).

4.2.3 | Near-top lower Siwalik horizon (orange)

The near-top lower Siwalik (orange) horizon shows comparable morphology to the sub-Cenozoic unconformity, though the surface is much shallower. Regionally, dramatic gradients in the slope of the near-top lower Siwalik reflection are rare. The surface displays regional northward deepening, progressing from southern highs between $-2,000$ and $-2,700$ m (Figure 7b) to northern depths of $-2,800$ to $-3,800$ m. However, this gradient is noticeably steeper in Block 10 and the Eastern Block (ca. 1.6°) when compared with the Western and Central Blocks (dip ca. 1.1°). Similar to the sub-Cenozoic unconformity, a regional depression ($-3,700$ m) is observed in the Eastern Block, and two smaller troughs are seen in the Western Block ($-3,100$ m; Figure 7b). The Western and Central Blocks are bridged longitudinally by a gently sloped structural high, which shallows to $-2,200$ m and spatially correlates with the Faizabad ridge. The horizon shallows in Block 10, reaching elevations of $-2,600$ to $-2,300$ m coinciding with the Munger-Saharsa ridge. It also shallows locally near the MFT. Elevations in the Deukhuri and Chitwan basins are comparable with those south of the MFT. However, the reflection is significantly shallower in the Dang basin, suggesting that it has been elevated by Sub-Himalayan thrust faulting. At the extreme southeast extremity of Block 10, a gentle fold extends between two steep strike-slip faults (Figure 6d). Duvall et al. (2020) interpret this feature as a fault-related fold above the blind OFT.

4.2.4 | Near-top middle Siwalik horizon (green)

Figure 7a shows the elevation of the near-top middle Siwalik (green) reflector. The surface varies regionally from $-1,000$ to $-1,700$ m. In comparison to underlying horizons, its structure is relatively uniform, reaching similar depths in all blocks. Regional northward deepening at 1° – 2° is again observed. A localized high in Block 10 coincides with the interpreted blind OFT at depth (Figures 6d and 7). Close to the MFT, in the Central and Western Blocks, this horizon shallows abruptly northward at steeper angles (dips 5° – 11°), probably due to tectonic wedging associated with the thrust front (Figure 6a). Deformation is also probably responsible for the higher elevation of this reflector in the Deukhuri and Dang intermontane basins, consistent with

inferences from balanced cross-sections (e.g. Hirschmiller et al., 2014), whereas the elevation of this reflector in the Chitwan basin is comparable to that in the Central Block to the south of the MFT. Regional high points at approximately $-1,200$ to -900 m are observed in portions of the Western Block. Along strike, regional low points ($-1,600$ to $-1,700$ m) occur in the centres of the Eastern, Central and Western Blocks. Local highs are seen at the eastern edge of the Western Block, corresponding to the western flank of the Faizabad ridge; and between the Eastern and Central Blocks. A gentle high corresponds to the western portion of the Munger-Saharsa ridge.

4.3 | Isopach map features

The four isopach intervals shown in Figure 8 correspond approximately to the upper Siwalik Group (Figure 8a); the middle Siwalik Group (Figure 8b); the lower foreland basin (Figure 8c); and the Vindhyan and Gondwanan successions (Figure 8d). The maps represent progressively longer time intervals from present to Proterozoic. In addition, because the topographic surface is everywhere near sea level, the structure map of the blue reflector (Figure 7d) closely approximates an isopach map of the entire stratified succession.

Figure 8d shows the stratigraphic thickness of the rock units between the acoustic basement (blue) and the sub-Cenozoic unconformity (pink), consisting mainly of Vindhyan, and possible Gondwanan strata. The thickness of this interval varies dramatically, from 0 to $>7,000$ m. The thickness is highly variable in the Eastern Block, related to the presence of normal faults, and onlap onto the basement (Figures 5c and 8d). The Vindhyan succession is absent in some portions of Block 10, and less than 1 km thick elsewhere. The interval is also less than 1 km thick at the east and west ends of the Western Block. This interval is appreciably thicker in the Gandak depression, and in a small trough in the centre of the Western Block.

The interval (Figure 8c) between the sub-Cenozoic unconformity (pink) and the near-top lower Siwalik horizon (orange) encompasses the lower Siwalik sub-Group, the Dumri Formation, and probably the Bhainskati Formation (and equivalents; Figure 2). The thickness of this interval ranges from ca. 2,800 m in the foredeep of the Western and Central Blocks, to <800 m in Block 10 (Figure 8c). The thicker values are significantly greater than the typical aggregate thicknesses recorded in the Sub-Himalaya (ca. 2,100 m), but the outcrop sections are truncated by faults. The section in Block 10 is clearly thinner than the corresponding strata exposed in the Sub-Himalaya. The interval appears to thicken both from south to north and from east to west (Figure 8c). Local thin

areas occur at the eastern edge of the Western Block and in Block 10 (Figure 8c).

The thickness of the near-top lower Siwalik (orange) to the near-top middle Siwalik (green) interval ranges from ca. 700 to 2,200 m (Figure 8b) (compared with typical sections of 2,100 m in the Sub-Himalaya). The interval thickens from ca. 600 to ca. 1,000 m from south to north. The interval also increases in thickness from east to west (Figure 8b). Three regional thin areas are seen: a thinning to >800 m in the westernmost part of the study area, thinning to >750 m in the western part of the Central Block, and an overall thinning along strike from the Eastern Block to Block 10 (Figure 8b). The Block 10 thin area covers a swath 145 km wide, directly over the Munger-Saharsa ridge. A subtler thickness gradient is seen in the Central Block, where ca. 500 m of thinning occurs over 45 km. Thickness reaches a maximum in the foredeep of the Eastern Block, correlating with the Gandak depression (Srinivasan & Khar, 1996).

The thickness between the near-top middle Siwalik and the topographic surface, encompassing the upper Siwalik Group, ranges from ca. 1,100 to 2,000 m (Figure 8a), compared with an estimate up to ca. 1,105 m derived from partial sections in the Sub-Himalaya (Mugnier et al., 1999). The Western Block contains the thickest and thinnest areas, the thinnest areas occurring close to the MFT. Elsewhere, the interval generally thickens northward, but notably shows a thickness minimum near the postulated Faizabad ridge (Figure 8a).

4.4 | Implications of thickness variations

The Siwalik Group represents predominantly fluvial environments comparable to that existing in the Ganga Plain at the present day, which shows minimal vertical relief over most of its area. As such, the reflections within the Siwalik Group are interpreted to represent surfaces that were close to base-level, and therefore approximately horizontal, at the time of deposition. A similar argument can be applied to the sub-Cenozoic unconformity, which is overlain, where observed, by shallow marine sediments. Hence the thicknesses of the packages of sediment between these surfaces primarily record accommodation space creation during sedimentation. Because of the great thickness of the Siwalik succession, the relative effects of eustatic change on accommodation are minor. Differential compaction effects are also likely to be relatively minor, but are predicted to have reduced the contrasts between thicker and thinner parts of any given interval. Hence, we interpret lateral and longitudinal thickness contrasts in Figure 8a–c to primarily reflect differential subsidence of the underlying basement during sediment accumulation.

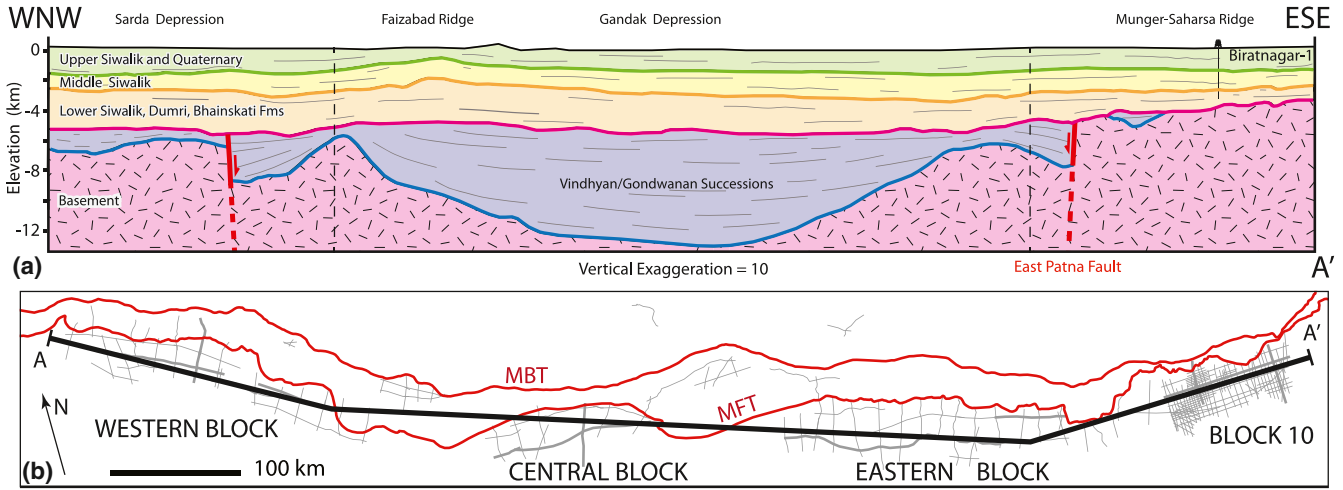


FIGURE 9 (a) Longitudinal vertically exaggerated profile A-A' spanning the Ganga Basin of Nepal from west to east. Vertical lines represent changes of profile direction. Basement faults from Godin and Harris (2014) have been projected on the profile. (b) Map shows line of section. MBT: Main Boundary Thrust; MFT: Main Frontal Thrust

4.5 | Geometry and development of the Ganga Basin

The structural and isopach maps generated from the seismic data display a regional geometry consistent with foreland basin models (Figures 7 and 8). A gentle northward deepening/thickening of Cenozoic horizons/intervals reflects a slope from the southern edge of the study area towards the foredeep. The Siwalik horizons are locally shallower along the northern extremities of the basin, reflecting the local influence of thrust faults and related folds near the MFT (Figures 6a and 7a,b).

Our data show that the geometry of the crystalline basement is highly irregular, and partly controlled by normal faults (e.g. Figures 5 and 8d). Much of this basement topography is filled by Vindhyan/Gondwanan sedimentary successions. However, highs in the sub-Cenozoic unconformity – roughly consistent with the location of the Munger-Saharsa and Faizabad ridges, act as major controls on foreland-basin accommodation across the basin. The Vindhyan/Gondwanan successions are regionally thinned above these ridges, or, in the case of the Munger-Saharsa ridge, discontinuous (Figure 8d). The western edge of the Munger-Saharsa ridge best spatially correlates to the East Patna Fault, while the Lucknow Fault marks the western boundary of the Faizabad ridge (Figure 9). Both these faults coincide with crustal-scale structures mapped by Godin and Harris (2014), but do not significantly offset the Cenozoic strata. The majority of the sub-Cenozoic strata are restricted to the intervening Gandak and Sarda depressions, where Vindhyan/Gondwanan successions occur in distinct basins while the sub-Cenozoic unconformity marks their upper boundary (Figure 8d). Small half-grabens of Vindhyan or Gondwanan strata occur on

and around the flanks of the Munger-Saharsa ridge (e.g. Figure 5c). The major ridges and depressions continue south into India (Raiverman, 1983; Raiverman et al., 1994; Shukla & Chakraborty, 1994; Srinivasan & Khar, 1996; Valdiya, 1976).

The sub-Cenozoic unconformity is a discrete horizon showing up to 15° of discordance between units above and below. Above the unconformity, the youngest foreland basin deposits gently undulate from NW to SE, relatively unperturbed by faults except around the two basement highs and close to the MFT (Figures 8a,b and 9). None of the major faults that control the basement ridges and the distribution of Vindhyan to Gondwanan strata appear produce significant offsets of this surface, suggesting that the structural features in the overlying Ganga Basin were dominantly controlled by flexure of the basement, rather than by fault reactivation.

The overall structural geometry of the Ganga Basin highlighted by our regional markers suggests that differential subsidence has played (and continues to play) a significant role in generating accommodation. All basement lows correspond to thick successions in the Cenozoic strata (Figures 8 and 9), whereas all basement highs also correspond with thinner overlying strata. Structural lows correlate with those seen in Indian seismic data (Raiverman et al., 1994). Thus the Gandak and Sarda depressions probably extend from the Indian continental interior up to (and likely beyond) the MFT (Raiverman et al., 1994).

Isopach maps representing the thicknesses of the foreland basin strata shed light on the timing of basement-influenced subsidence. The two deepest Cenozoic intervals (between the sub-Cenozoic unconformity and the near-top middle Siwalik surface) show the most substantial changes along-strike (Figure 8b). They are thickest in the Gandak and Sarda

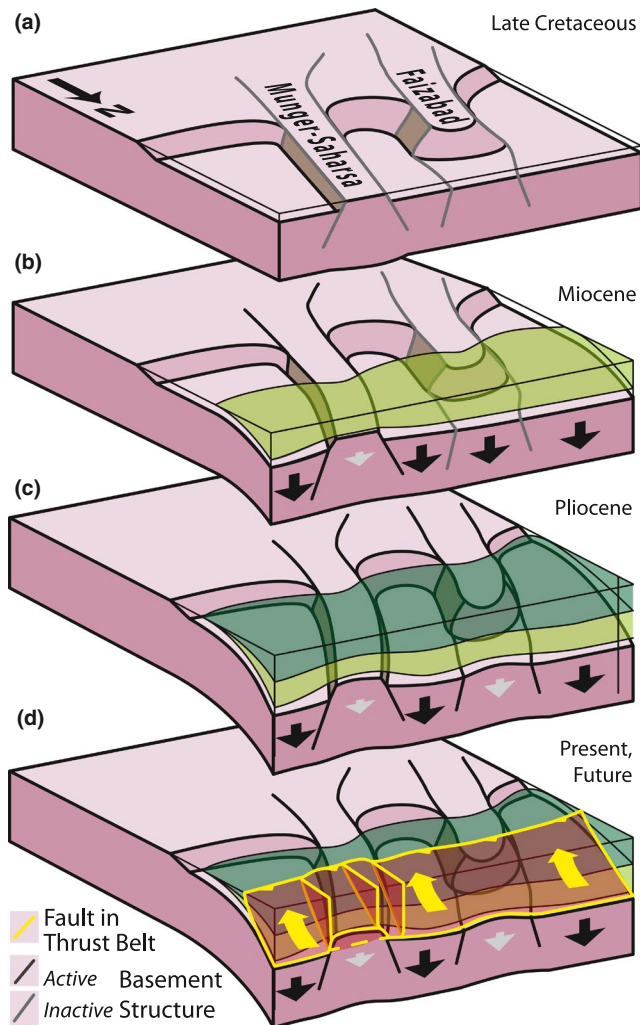


FIGURE 10 Conceptual cartoon showing along-strike thickness variations in the Ganga Basin. Not to scale. Foreland basin fill shown in green. Relative subsidence rates are shown schematically by black (faster) and grey (slower) arrows. (a) Ridges and basins in the Indian plate prior to Himalayan collision. (b) Flexure of plate under loading by orogen (not shown) leads to progressive differential subsidence of basin. During deposition of the lower Siwalik Group, the Munger-Saharsa ridge acts as an upwarp, and restricts deposition above. (c) During deposition of the middle and upper Siwalik Group, the Faizabad ridge shows increasing upwarp, while the Munger-Saharsa ridge shows less influence on subsidence. (d) Schematic representation of present-day and possible future faults (yellow), showing propagation of thrust front into the foreland basin, development of tear faults, and potential basement faults analogous to those seen in the Lesser Himalaya

depressions, where thicknesses approach three times that above the Munger-Saharsa ridge. These intervals also thin above local highs of the Western Block. We infer that the Cenozoic successions are similarly thin above the Faizabad ridge, although the data density is low in this region. These thickness trends are gradual. Overall, the thickness variation in the foreland basin strata indicates these depressions were subsiding at least as

recently as middle Siwalik deposition, but this differential subsidence likely continues to the present day (Figure 8a).

The spatial distribution of basement ridges and depressions identified in this study can be compared with those postulated by previous works (Godin & Harris, 2014; Raiverman et al., 1994). In Block 10 and the Eastern Block, the Munger-Saharsa ridge correlates well with previous estimates of its position based on satellite gravity data (e.g. Godin & Harris, 2014). However, Figure 7 shows that the western edge of this ridge closely correlates to the East Patna Fault, farther west than the position shown by Godin and Harris (2014). As illustrated in the isopach maps (Figure 8) the effect of this ridge decreases up section, suggesting that control by the Munger-Saharsa ridge was most important during the early stages of foreland basin subsidence.

A dramatic depression in the western half of the Eastern Block corresponds to the Gandak depression (e.g. Raiverman, 2002). A portion of this depression is also preserved beneath the Chitwan Dun basin, north of the MFT within the thrust belt (Figure 7c,d). The western margin of the Gandak depression, marking the eastern edge of the Faizabad ridge and associated faults (Godin & Harris, 2014; Godin et al., 2019) is complex. A thick Vindhyan basin, centred under the western part of the Central Block, thins westward towards a prominent positive feature near the eastern edge of the Western Block, approximately ca. 100 km west of the approximated ridge trace and associated structures (Godin & Harris, 2014; Godin et al., 2019). The sub-Cenozoic unconformity shows at most a minor positive feature centered slightly west of the Godin and Harris (2014) position. However, higher Siwalik surfaces suggest distinct upwarp across the postulated ridge. Isopach maps and the regional cross-section (Figures 8 and 9) show that most of the upwarp was acquired during the deposition of the upper Siwalik Group. This leads us to infer that the influence of the Faizabad Ridge on subsidence has increased over time.

5 | DISCUSSION

5.1 | Controls on basin subsidence

How have these basement heterogeneities controlled subsidence in the Ganga Basin? Deep-seated lineaments parallel to the edges of the Delhi-Haridwar, Faizabad, and Munger-Saharsa ridges represent surfaces that extend as deep as the base of the Indian lithosphere (Godin & Harris, 2014), and in the case of several ridges, appear to show opposing senses of dip. Several mapped basement faults align with these lineaments, including the Great Boundary, Lucknow, Kishangang, and West/East Patna Faults (Godin & Harris, 2014; Rao et al., 2015; Valdiya, 1976). Some of these faults have been

interpreted to be active based on observations of recent soft sediment deformation structures (e.g. Verma et al., 2017). Slip along these basement faults could provide a mechanism for the subsidence seen in the intervening basins. However, there are no significant offsets of the Cenozoic package along ridge margins at the present day, where the Cenozoic succession of the foreland basin smoothly tapers from basins onto neighbouring ridges (Figures 9 and 10c).

Therefore, we infer that the basement and ridges control the subsidence of the Ganga basin by affecting the flexural behaviour of the Indian Plate, as shown schematically in Figure 10a–c. Ridges behaved more stiffly under the advancing load of the Himalaya, subsiding less, while the intervening basins, inherited from the Proterozoic development of the Vindhyan basins, were more easily flexed and show greater subsidence.

5.2 | Flexural behaviour of the Indian lithosphere

To test whether the basement ridges and depressions could account for the differential subsidence observed in the foreland basin in this way, we model the flexure of the Indian Plate in two dimensions, in profiles perpendicular to the Himalayan front. This model setup is based upon the observation that the lateral thickness variations in the Cenozoic basin are of order ca. 1.5 km (Figure 9), approximately 30% of the maximum basin depth, and these differences occur over lateral distances of ca. 300 km. The resulting stresses are therefore roughly one fifth of those induced by the ca. 5 km depth of the foreland basin over an across-strike distance of ca. 200 km, as the Indian plate underthrusts Tibet (assuming an elastic rheology). We are therefore able to approximate the force balance as two-dimensional, without needing to model the stresses transmitted parallel to the strike of the foreland basin. We use a ‘broken plate’ model to simulate the flexure, as is common in foreland basin settings (e.g. Lyon-Caen & Molnar, 1985; McKenzie & Fairhead, 1997). For simplicity, we neglect the bending moment exerted on the end of the plate, and consider only the vertical load represented by the Himalaya and Tibetan Plateau. Due to our approach (below) of interpreting relative lateral variations in the flexural subsidence close to the orogen, and not the absolute magnitudes of this value, this assumption has no significant effect on our results. As described by Turcotte and Schubert (2014, equations 3.72, 3.127 and 3.141), the maximum amplitude of the flexural subsidence is given by

$$w_0 = \frac{V\alpha^3}{4D}$$

where V is the size of the load. α is the flexural parameter, and is given by

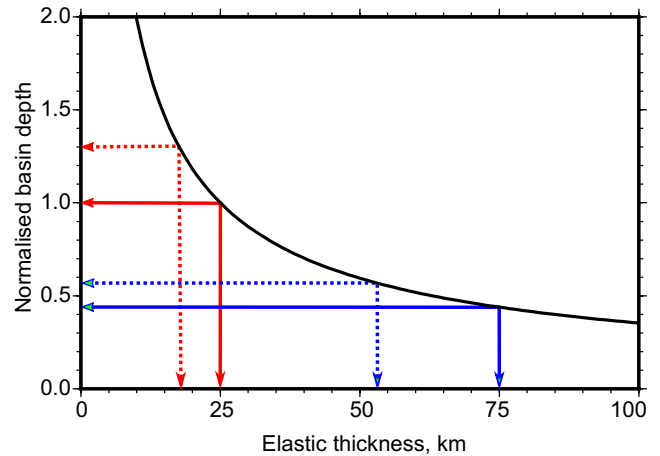


FIGURE 11 Relationship between elastic thickness and basin depth, for a fixed size of load. The basin depth is normalised to the value for an elastic thickness of 25 km, which therefore has a value of 1 on the vertical axis. This normalisation removes the absolute magnitude of the load from the analysis. The red and blue arrows show the lateral variations in elastic thickness that would be required to reproduce the factor of 1.3 lateral variations in Cenozoic sediment thickness, for values in the lower and higher range of previously suggested elastic thicknesses. For a plate with 25 km elastic thickness (red), a low-strength Proterozoic or Gondwanan sedimentary basin 8 km deep could account for the observed 30% increase in the flexural subsidence. For a 75 km elastic thickness of the plate (blue), a larger variation in crustal thickness (>20 km) is required, implying deeper rheology contrasts

$$\alpha = \left[\frac{4D}{(\rho_m - \rho_i)g} \right]^{1/4}$$

where ρ_m is the density of the mantle, ρ_i is the density of the basin infill, and g is the acceleration due to gravity. D is the flexural rigidity, and is given by

$$D = \frac{ET^3}{12(1-\nu^2)}$$

where E is Young's modulus, T is the elastic thickness, and ν is Poisson's ratio. See Turcotte and Schubert (2014) for details of the derivations of these expressions. By assuming that the load on the plate is constant along-strike, we can isolate the effects of lateral variations in elastic thickness in controlling the foreland subsidence. In order to remove the effects of the unknown total magnitude of the loading, we normalise the calculated foreland flexural displacements to the value for an arbitrarily-chosen elastic thickness (25 km), meaning that lateral variations in basin subsidence can be linked to lateral variations in elastic thickness.

Figure 11 shows the results of these calculations. The curve shows that the maximum flexural displacement varies as the elastic thickness raised to the power of $(-3/4)$. This result can be understood by simple scaling arguments. As seen in the equations above, the maximum subsidence in a flexural basin is proportional to the cube of the flexural parameter, and inversely proportional to the flexural rigidity. The flexural parameter is itself proportional to the flexural rigidity to the power $1/4$. Therefore, the flexural subsidence is proportional to the flexural rigidity to the power of $(-1/4)$, and given that the flexural rigidity depends on the cube of the elastic thickness, the total flexural displacement is proportional to the elastic thickness to the power $(-3/4)$. All other parameters tradeoff against each other (e.g. size of load, densities of the mantle and basin infill, Poisson's ratio, and Young's modulus), and affect the amplitude of deflection of the plate. However, by assuming that these quantities do not vary along strike, we can focus on the along-strike variation in elastic thickness required to reproduce the observed along-strike variation in the amplitude of flexure. An along-strike variation in basin depth of a factor of 1.3, similar to that seen in the Ganga Basin would require along-strike variations in the elastic thickness of a factor of ca. 1.4. Thus, if the elastic thickness over the basement ridges were 25 km, an elastic thickness beneath the Vindhyan basins of ca. 18 km would be required to cause the observed thickness variations (red lines on Figure 11). If the elastic thickness under the basement ridges were 75 km, an elastic thickness under the Vindhyan basins of ca. 53 km would be required to match the sedimentary thickness variations (blue lines on Figure 11).

Are lateral elastic thickness variations of this type plausible, and can this mechanism therefore explain the along-strike variations in sediment thickness? The actual elastic thickness of the Indian plate is a source of long-running debate, suggestions ranging from less than 30 km to over 100 km (e.g. Bilham et al., 2003; Jordan & Watts, 2005; Karner & Watts, 1983; Lyon-Caen & Molnar, 1985; Maggi et al., 2000; McKenzie & Fairhead, 1997). Much of the debate has centred around (1) whether the location of the 'plate break' is fixed in the inversions when using space-domain methods, and (2) the methodologies used for frequency-domain estimates, and whether these represent true estimates or upper bounds. Detailed discussion of these issues can be found in Jackson et al. (2008) and McKenzie et al. (2014). Here our concern is not with the absolute value of the elastic thickness, but with possible lateral variations. There is an ca. 8 km lateral variation in the thickness of the Vindhyan/Gondwanan sediments shown in Figure 9. If these sedimentary rocks are weaker than the underlying crystalline basement, then they would yield kilometre-scale lateral variations in the elastic thickness of up to 8 km (if the sedimentary rocks were supporting none of the flexural stresses). The presence of an 8 km deep basin also implies a crustal thickness contrast between the regions,

in order to have generated the accommodation for these sediments during deposition. These lateral variations would also be expected to produce an along-strike variation in elastic thickness. If the average elastic thickness is as low as the 25–32 km suggested by McKenzie et al. (2014), then a pre-existing strength contrast between the basement ridges and the basins could generate the along-strike variations in elastic thickness required to reproduce the Cenozoic sediment thickness contrasts. If the average elastic thickness were higher, as suggested by Jordan and Watts (2005), then additional along-strike strength contrasts, presumably related to the deeper crustal or lithosphere structure, would be required in order to reproduce the observed sedimentary thickness variations (e.g. related to thinning at depth during basin formation). Both these situations are plausible, suggesting that the along-strike changes in the Cenozoic sediment thickness can indeed be explained by pre-existing strength (elastic thickness) contrasts within the Indian plate, which control the amount of flexural subsidence due to loading by the Himalaya.

5.3 | Behaviour of the basement ridges within the Himalayan orogen

Thrusts in the foreland basin and in the Sub-Himalaya are predominantly thin-skinned and therefore only incorporate foreland basin sedimentary rocks into thrust sheets. However, in the Lesser Himalaya substantial sections of Vindhyan and Gondwanan strata are involved in the belt, showing major along-strike variations (Figure 1b) that define lateral ramps, fenster, and klippen. Therefore, we infer that as the relatively upstanding ridges are drawn into the thrust belt, they are more easily decapitated by advancing thrusts than the intervening depressions, producing lateral ramp-flat geometries in the Lesser and Greater Himalaya as documented by Soucy La Roche and Godin (2019) and DeCelles et al. (2020). Figure 10d schematically shows the propagation of thrusts and tear faults into the foreland basin as seen at the present day, together with potential future faults that may incorporate basement into the thrust belt and propagate through the Indian lithosphere slab as envisaged by Chen et al. (2015). The structures documented beneath the foreland basin therefore provide a powerful tool for understanding lateral variations in structure within the orogen.

6 | CONCLUSIONS

Newly available seismic data have allowed us to evaluate previously unknown longitudinal changes in geometry (Figure 7) and thicknesses (Figure 8) of sedimentary successions within the Ganga foreland basin. Cenozoic deposition has been influenced by several fault-bounded

crustal-scale structures, oriented at a high angle to the strike of the Himalaya. Basement highs, such as the Faizabad and Munger-Saharsa ridges, broadly correlate with depositional minima in overlying strata. In intervening depressions, significant Vindhyan and Cenozoic strata have been accommodated in structural lows. Thickness variations in the sedimentary package above suggest that these basement structures affected the flexural thickness of the Indian lithosphere through much of the Cenozoic, leading to along-strike segmentation of the foreland basin. This segmentation has not only controlled the thickness and geometry of sedimentary sequences deposited, but also the localization of wrench and thrust faults associated with the Himalayan thrust front (Figure 10). The Munger-Saharsa ridge shows declining influence through time, from the lower to the upper Siwalik Group. In contrast, the Faizabad ridge was most prominent during Middle Siwalik deposition. Taken together, these observations are interpreted to show differential subsidence resulting from variations in flexural rigidity of the Indian Plate. We have tested this hypothesis, using a simple flexural model to show that the observed variations in subsidence are consistent with the depths of the Proterozoic (Vindhyan) basins and the heights of the intervening ridges, and with reasonable values for the flexural thickness of Indian lithosphere. Tear faults, at high angles to the thrust front, have previously been interpreted as the result of reactivation of ridge-bounding faults at depth (e.g. Paul et al., 2015). Our interpretation of the seismic data, together with that of Duvall et al. (2020), suggests that their localization is related to thrust propagation over the basement ridges and reflects indirect controls by the ridges on the behaviour of the overlying foreland basin strata (Figure 10). However, once involved in the thrust belt, the basement ridges more directly control the development of the orogen, as demonstrated by Soucy La Roche and Godin (2019). These results show that lower-plate structures at high angles to orogens can have profound effects on orogen development, inducing non-cylindrical features from the foreland basin to high structural levels in the thrust belt.

ACKNOWLEDGEMENTS

The authors thank John Clayburn and Cairn Energy for their contribution to the project. Schlumberger's Petrel software licenses donated to the University of Alberta assisted data analysis. Participation by JWFW and LG was supported by National Sciences and Engineering Research Council of Canada Discovery Grants. Dawa Tamang, Pradip Tamang, and Alison Martin assisted in the field. We are grateful to journal reviewers Sam Haines and Lucia Torrado, and to associate editor Craig Magee, for their insightful comments, which led to significant improvements in the paper. We acknowledge the use of public geological data from the United

States Geological Survey database, accessed from: <https://catalog.data.gov/dataset/geologic-map-of-south-asia-geo8ag>.

CONFLICT OF INTEREST

The authors declared no conflicts of interest.

AUTHOR CONTRIBUTIONS

LG and JWFW conceived the project. YN acquired access to the data. MD interpreted the data under the supervision of JWFW and wrote the first draft of the paper. MJD, JWFW, LG, and YN carried out fieldwork together. AC performed flexural subsidence analysis and wrote the first draft of that section. All five authors contributed edits to the paper.

PEER REVIEW

The peer review history for this article is available at <https://publons.com/publon/10.1111/bre.12584>.

DATA AVAILABILITY STATEMENT

The data that support the findings of this study are available from Cairn Energy. Restrictions apply to the availability of SEG-Y data which were used under license for this study. Data are available from the authors with the permission of Cairn Energy. Images of the data in Figures S5 and S6 are provided in the Supplementary Information.

ORCID

Michael J. Duvall  <https://orcid.org/0000-0001-5269-3134>

John W. F. Waldron  <https://orcid.org/0000-0002-1401-8848>

Laurent Godin  <https://orcid.org/0000-0003-1639-3550>

Yani Najman  <https://orcid.org/0000-0003-1286-6509>

Alex Copley  <https://orcid.org/0000-0003-0362-0494>

REFERENCES

- Aditya, S., Raju, A. T. R., & Shukla, S. N. (1979). Assessment of Hydrocarbon Prospects of the sub-Himalayan, Punjab and Ganga basins-India. In *Himalayan Geology Seminar New Delhi 1976: Section 3 - Oil and natural gas resources* (Vol. 41, pp. 127–140). Geological Survey of India Miscellaneous Publications.
- Almeida, R. V., Hubbard, J., Liberty, L., Foster, A., & Sapkota, S. N. (2018). Seismic imaging of the Main Frontal Thrust in Nepal reveals a shallow décollement and blind thrusting. *Earth and Planetary Science Letters*, 494, 216–225. <https://doi.org/10.1016/j.epsl.2018.04.045>
- Anders, A. M., Roe, G. H., Hallet, B., Montgomery, D. R., Finnegan, N. J., & Putkonen, J. (2006). Spatial patterns of precipitation and topography in the Himalaya. In S. D. Willett, N. Hovius, M. T. Brandon, & D. M. Fisher (Eds.), *Tectonics, climate, and landscape evolution* (Vol. 398, pp. 39–53). Geological Society of America Special Paper. [https://doi.org/10.1130/2006.2398\(03\)](https://doi.org/10.1130/2006.2398(03))

- Appel, E., Rösler, W., & Corvinus, G. (1991). Magnetostratigraphy of the Miocene-Pleistocene Surai Khola Siwaliks in West Nepal. *Geophysical Journal International*, 105(1), 191–198. <https://doi.org/10.1111/j.1365-246X.1991.tb03455.x>
- Avouac, J.-P. (2003). Mountain building, erosion, and the seismic cycle in the Nepal Himalaya. In *Advances in geophysics* (Vol. 46). Elsevier. [https://doi.org/10.1016/S0065-2687\(03\)46001-9](https://doi.org/10.1016/S0065-2687(03)46001-9)
- Balakrishnan, T. S., Unnikrishnan, P., & Murty, A. V. S. (2009). The tectonic map of India and contiguous areas. *Journal of the Geological Society of India*, 74(2), 158–168. <https://doi.org/10.1007/s12594-009-0119-4>
- Bashyal, R. P. (1998). Petroleum exploration in Nepal. *Journal of Nepal Geological Society*, 18, 19–24. <https://doi.org/10.3126/jngs.v18i0.32193>
- Basuyau, C., Diament, M., Tiberi, C., Hetényi, G., Vergne, J., & Peyrefitte, A. (2013). Joint inversion of teleseismic and GOCE gravity data: Application to the Himalayas. *Geophysical Journal International*, 193(1), 149–160. <https://doi.org/10.1093/gji/ggs110>
- Bernet, M., van der Beek, P., Pik, R., Huyghe, P., Mugnier, J.-L., Labrin, E., & Szulc, A. (2006). Miocene to Recent exhumation of the central Himalaya determined from combined detrital zircon fission-track and U/Pb analysis of Siwalik sediments, western Nepal: Miocene to Recent exhumation of the central Himalaya. *Basin Research*, 18(4), 393–412. <https://doi.org/10.1111/j.1365-2117.2006.00303.x>
- Bhattacharyya, A. (1996). *Recent advances in Vindhyan geology* (Vol. 36). Geological Society of India Memoir.
- Bilham, R., Bendick, R., & Wallace, K. (2003). Flexure of the Indian plate and intraplate earthquakes. *Journal of Earth System Science*, 112(3), 315–329. <https://doi.org/10.1007/BF02709259>
- Biswas, S. K. (1999). A review on the evolution of rift basins in India during Gondwana with special reference to western Indian basins and their hydrocarbon prospects. *Proceedings of the Indian National Science Academy - Part A*, 65, 261–284.
- Bollinger, L., Avouac, J. P., Beyssac, O., Catlos, E. J., Harrison, T. M., Grove, M., Goffé, B., & Sapkota, S. (2004). Thermal structure and exhumation history of the Lesser Himalaya in central Nepal: Thermal structure of the Lesser Himalaya. *Tectonics*, 23(5), TC5015. <https://doi.org/10.1029/2003TC001564>
- Bose, P. K., Sarkar, S., Das, N. G., Banerjee, S., Mandal, A., & Chakraborty, N. (2015). Proterozoic Vindhyan basin: Configuration and evolution. In R. Mazumder, & P. G. Eriksson (Eds.), *Precambrian basins of India: Stratigraphic and tectonic context* (Vol. 43, pp. 85–102). Geological Society of London Memoir.
- Bouilhol, P., Jagoutz, O., Hanchar, J. M., & Dudas, F. O. (2013). Dating the India-Eurasia collision through arc magmatic records. *Earth and Planetary Science Letters*, 366, 163–175. <https://doi.org/10.1016/j.epsl.2013.01.023>
- Brown, L. D., Zhao, W., Nelson, K. D., Hauck, M., Alsdorf, D., Ross, A., Cogan, M., Clark, M., Liu, X., & Che, J. (1996). Bright spots, structure, and magmatism in southern Tibet from INDEPTH seismic reflection profiling. *Science*, 274(5293), 1688–1690. <https://doi.org/10.1126/science.274.5293.1688>
- Burbank, D. W., Beck, R. A., & Mulder, T. (1996). The Himalayan foreland basin. In A. Yin & T. M. Harrison (Eds.), *The tectonic evolution of Asia* (pp. 149–188). Cambridge University Press.
- Burchfiel, B. C., Zhiliang, C., Hodges, K. V., Yuping, L., Royden, L. H., & Changrong, D. (1992). *The South Tibetan Detachment System, Himalayan Orogen: Extension Contemporaneous with and Parallel to Shortening in a Collisional Mountain Belt* (Vol. 269). Geological Society of America - Special Paper.
- Burgess, W., Yin, A., Dubey, C. S., Shen, Z.-K., & Kelty, T. K. (2012). Holocene shortening across the Main Frontal Thrust zone in the eastern Himalaya. *Earth and Planetary Science Letters*, 357–358, 152–167. <https://doi.org/10.1016/j.epsl.2012.09.040>
- Casshyap, S. M., & Khan, A. (2000). Basin of central India: Evidence of pre-Trap doming, rifting and palaeoslope reversal. *Journal of African Earth Sciences*, 31(1), 65–76.
- Cawood, P. A., Johnson, M. R., & Nemchin, A. A. (2007). Early Palaeozoic orogenesis along the Indian margin of Gondwana: Tectonic response to Gondwana assembly. *Earth and Planetary Science Letters*, 255, 70–84. <https://doi.org/10.1016/j.epsl.2006.12.006>
- Chatterjee, N., & Ghose, N. C. (2011). Extensive Early Neoproterozoic high-grade metamorphism in North Chotanagpur Gneissic Complex of the Central Indian Tectonic Zone. *Gondwana Research*, 20(2–3), 362–379. <https://doi.org/10.1016/j.gr.2010.12.003>
- Chen, Y., Li, W., Yuan, X., Badal, J., & Teng, J. (2015). Tearing of the Indian lithospheric slab beneath southern Tibet revealed by SKS-wave splitting measurements. *Earth and Planetary Science Letters*, 413, 13–24. <https://doi.org/10.1016/j.epsl.2014.12.041>
- Cohen, K. M., Harper, D. A. T., Gibbard, P. L., & Fan, J.-X. (2013). The ICS international chronostratigraphic chart v2018/08. *Episodes*, 36, 119–204. <https://doi.org/10.18814/epiiugs/2013/v36i3/002>
- Corvinus, G., & Rimal, L. N. (2001). Biostratigraphy and geology of the Neogene Siwalik Group of the Surai Khola and Rato Khola areas in Nepal. *Palaeogeography, Palaeoclimatology, Palaeoecology*, 165(3), 251–279. [https://doi.org/10.1016/S0031-0182\(00\)00163-2](https://doi.org/10.1016/S0031-0182(00)00163-2)
- Dasgupta, S. (1993). Tectono-geologic framework of the eastern Gangetic foredeep. In *Bihar Nepal earthquake (August 20, 1988)* (Vol. 31, pp. 61–69). Geological Survey of India Special Publication.
- Dasgupta, S., Mukhopadhyay, B., Mukhopadhyay, M., & Nandy, D. R. (2013). Role of transverse tectonics in the Himalayan collision: Further evidences from two contemporary earthquakes. *Journal of the Geological Society of India*, 81(2), 241–247. <https://doi.org/10.1007/s12594-013-0027-5>
- de la Torre, T. L., Monsalve, G., Sheehan, A. F., Sapkota, S., & Wu, F. (2007). Earthquake processes of the Himalayan collision zone in eastern Nepal and the southern Tibetan Plateau. *Geophysical Journal International*, 171(2), 718–738. <https://doi.org/10.1111/j.1365-246X.2007.03537.x>
- DeCelles, P. G., Carrapa, B., Ojha, T. P., Gehrels, G. E., & Collins, D. (2020). Structural and thermal evolution of the Himalayan thrust belt in midwestern Nepal. In P. G. DeCelles, B. Carrapa, T. P. Ojha, G. E. Gehrels, & D. Collins (Eds.), *Structural and thermal evolution of the Himalayan thrust belt in midwestern Nepal* (pp. 1–79). Geological Society of America. [https://doi.org/10.1130/2020.2547\(01\)](https://doi.org/10.1130/2020.2547(01))
- DeCelles, P. G., Gehrels, G. E., Najman, Y., Martin, A. J., Carter, A., & Garzanti, E. (2004). Detrital geochronology and geochemistry of Cretaceous-Early Miocene strata of Nepal: Implications for timing and diachroneity of initial Himalayan orogenesis. *Earth and Planetary Science Letters*, 227(3–4), 313–330. <https://doi.org/10.1016/j.epsl.2004.08.019>
- DeCelles, P. G., Gehrels, G. E., Quade, J., & Ojha, T. P. (1998). Eocene-early Miocene foreland basin development and the history of Himalayan thrusting, western and central Nepal. *Tectonics*, 17(5), 741–765. <https://doi.org/10.1029/98TC02598>
- DeCelles, P. G., Gehrels, G. E., Quade, J., Ojha, T. P., Kapp, P. A., & Upreti, B. N. (1998). Neogene foreland basin deposits, erosional unroofing, and the kinematic history of the Himalayan fold-thrust belt, western Nepal. *Geological Society of America Bulletin*, 110(1), 2–21. [https://doi.org/10.1130/0016-7606\(1998\)110<0002:NFBDEU>2.3.CO;2](https://doi.org/10.1130/0016-7606(1998)110<0002:NFBDEU>2.3.CO;2)

- Dhital, M. R. (2015). *Geology of the Nepal Himalaya*. Regional Geology Reviews. Springer.
- Duncan, C., Masek, J., & Fielding, E. (2003). How steep are the Himalaya? Characteristics and implications of along-strike topographic variations. *Geology*, 31(1), 75–78. [https://doi.org/10.1130/0091-7613\(2003\)031<0075:HSATHC>2.0.CO;2](https://doi.org/10.1130/0091-7613(2003)031<0075:HSATHC>2.0.CO;2)
- Duvall, M. J., Waldron, J. W. F., Godin, L., & Najman, Y. (2020). Active strike-slip faults and an outer frontal thrust in the Himalayan foreland basin. *Proceedings of the National Academy of Sciences*, 117(30), 17615–17621. <https://doi.org/10.1073/pnas.2001979117>
- Fuloria, R. C. (1996). Geology and hydrocarbon prospects of the Vindhyan sediments in Ganga valley. *Memoirs of the Geological Society of India*, 36, 235–256.
- Gahalaut, V. K., & Kundu, B. (2012). Possible influence of subducting ridges on the Himalayan arc and on the ruptures of great and major Himalayan earthquakes. *Gondwana Research*, 21(4), 1080–1088. <https://doi.org/10.1016/j.gr.2011.07.021>
- Gansser, A. (1964). *Geology of the Himalayas*. Interscience Publishers.
- Garzanti, E. (2019). The Himalayan Foreland Basin from collision onset to the present: A sedimentary–petrology perspective. In P. J. Treloar, & M. P. Searle (Eds.), *Himalayan tectonics: A modern synthesis* (Vol. 483). Geological Society of London Special Publications.
- Gautam, P., & Fujiwara, Y. (2000). Magnetic polarity stratigraphy of Siwalik Group sediments of Karnali River section in western Nepal. *Geophysical Journal International*, 142(3), 812–824. <https://doi.org/10.1046/j.1365-246x.2000.00185.x>
- Godin, L., & Harris, L. B. (2014). Tracking basement cross-strike discontinuities in the Indian crust beneath the Himalayan orogen using gravity data – Relationship to upper crustal faults. *Geophysical Journal International*, 198(1), 198–215. <https://doi.org/10.1093/gji/ggu131>
- Godin, L., Soucy La Roche, R., Waffle, L., & Harris, L. B. (2019). Influence of inherited Indian basement faults on the evolution of the Himalayan Orogen. In *Crustal architecture and evolution of the Himalaya–Karakoram–Tibet Orogen* (Vol. 481, pp. 251–276). Special Publication - Geological Society of London.
- Goscombe, B., Gray, D., & Foster, D. A. (2018). Metamorphic response to collision in the Central Himalayan Orogen. *Gondwana Research*, 57, 191–265. <https://doi.org/10.1016/j.gr.2018.02.002>
- Grujic, D., Coutand, I., Doon, M., & Kellett, D. A. (2017). Northern provenance of the Gondwana Formation in the Lesser Himalayan Sequence: Constraints from 40Ar/39Ar dating of detrital muscovite in Darjeeling–Sikkim Himalaya, Indian. *Journal of Geosciences*, 136, 15–27. <https://doi.org/10.3301/IJG.2015.28>
- Hartsink, J., & Pradhan, U. M. S. (1989). *Well completion report - Biratnagar 1*. Shell Nepal B.V.
- Hauck, M. L., Nelson, K. D., Brown, L. D., Zhao, W., & Ross, A. R. (1998). Crustal structure of the Himalayan orogen at ~90 east longitude from Project INDEPTH deep reflection profiles. *Tectonics*, 17(4), 481–500. <https://doi.org/10.1029/98TC01314>
- Heim, A., & Gansser, A. (1939). *Central Himalaya - Geological observations of the Swiss expedition 1936*. Hindustan Publishing.
- Hirschmiller, J., Grujic, D., Bookhagen, B., Coutand, I., Huyghe, P., Mugnier, J.-L., & Ojha, T. (2014). What controls the growth of the Himalayan foreland fold-and-thrust belt? *Geology*, 42(3), 247–250. <https://doi.org/10.1130/G35057.1>
- Hu, X., Wang, J., BouDagher-Fadel, M., Garzanti, E., & An, W. (2016). New insights into the timing of the India – Asia collision from the Paleogene Quixia and Jialazi formations of the Xigaze forearc basin, South Tibet. *Gondwana Research*, 32, 76–92. <https://doi.org/10.1016/j.gr.2015.02.007>
- Hughes, N. C., Peng, S., Bhargava, O. N., Ahluwalia, A. D., Walia, S., Myrow, P. M., & Parcha, S. K. (2005). Cambrian biostratigraphy of the Tal Group, Lesser Himalaya, India, and early Tsanglangpau (late early Cambrian) trilobites from the Nigali Dhar syncline. *Geological Magazine*, 142(1), 57–80. <https://doi.org/10.1017/S0016756804000366>
- Husson, L., & Mugnier, J.-L. (2003). Three-dimensional horizon reconstruction from outcrop structural data, restoration, and strain field of the Baisahi anticline, Western Nepal. *Journal of Structural Geology*, 25, 79–90. [https://doi.org/10.1016/S0191-8141\(02\)00044-5](https://doi.org/10.1016/S0191-8141(02)00044-5)
- Jackson, J., McKenzie, D. P., Priestley, K., & Emmerson, B. (2008). New views on the structure and rheology of the lithosphere. *Journal of the Geological Society*, 165(2), 453–465. <https://doi.org/10.1144/0016-76492007-109>
- Jordan, T., & Watts, A. (2005). Gravity anomalies, flexure and the elastic thickness structure of the India-Eurasia collisional system. *Earth and Planetary Science Letters*, 236(3–4), 732–750. <https://doi.org/10.1016/j.epsl.2005.05.036>
- Karner, G. D., & Watts, A. B. (1983). Gravity anomalies and flexure of the lithosphere at mountain ranges. *Journal of Geophysical Research: Solid Earth*, 88(B12), 10449–10477. <https://doi.org/10.1029/JB088iB12p10449>
- Karunakaran, C., & Rao, A. R. (1979). Status of exploration for hydrocarbons in the Himalayan region—contributions to stratigraphy and structure. In *Himalayan Geology Seminar New Delhi 1976: Section 3 – Oil and natural gas resources* (Vol. 41, pp. 1–66). Geological Survey of India Miscellaneous Publications.
- Kellett, D. A., Cottle, J. M., & Larson, K. P. (2019). The South Tibetan Detachment System: History, advances, definition and future directions. In *Himalayan tectonics: A modern synthesis* (p. 483). Geological Society London Special Publications.
- Kellett, D. A., & Grujic, D. (2012). New insight into the South Tibetan detachment system: Not a single progressive deformation. *Tectonics*, 31(2), A2007. <https://doi.org/10.1029/2011TC002957>
- Krishnan, M. S. (1949). *Geology of India and Burma*. Madras Law Journal Office.
- Kumar, R., & Tandon, S. K. (1985). Sedimentology of Plio-Pleistocene Late orogenic deposits associated with intraplate subduction—The Upper Siwalik Subgroup of a part of Panjab Sub-Himalaya, India. *Sedimentary Geology*, 42(1–2), 105–158. [https://doi.org/10.1016/0037-0738\(85\)90076-4](https://doi.org/10.1016/0037-0738(85)90076-4)
- Lyon-Caen, H., & Molnar, P. (1985). Gravity anomalies, flexure of the Indian plate, and the structure, support and evolution of the Himalaya and Ganga Basin. *Tectonics*, 4(6), 513–538. <https://doi.org/10.1029/TC004i006p00513>
- Maggi, A., Jackson, J. A., McKenzie, D., & Priestley, K. (2000). Earthquake focal depths, effective elastic thickness, and the strength of the continental lithosphere. *Geology*, 28(6), 495–498. [https://doi.org/10.1130/0091-7613\(2000\)28<495:EFDEET>2.0.CO;2](https://doi.org/10.1130/0091-7613(2000)28<495:EFDEET>2.0.CO;2)
- Mathur, N. S. (1978). Biostratigraphical aspects of the Subathu Formation, Kumaun Himalaya. *Recent Researches in Geology*, 5, 96–112.
- McKenzie, D., & Fairhead, D. (1997). Estimates of the effective elastic thickness of the continental lithosphere from Bouguer and free air gravity anomalies. *Journal of Geophysical Research: Solid Earth*, 102(B12), 27523–27552. <https://doi.org/10.1029/97JB02481>
- McKenzie, D., Yi, W., & Rummel, R. (2014). Estimates of Te from GOCE data. *Earth and Planetary Science Letters*, 399, 116–127. <https://doi.org/10.1016/j.epsl.2014.05.003>
- McKenzie, N. R., Hughes, N. C., Myrow, P. M., Xiao, S., & Sharma, M. (2011). Correlation of Precambrian-Cambrian sedimentary

- successions across northern India and the utility of isotopic signatures of Himalayan lithotectonic zones. *Earth and Planetary Science Letters*, 312(3–4), 471–483. <https://doi.org/10.1016/j.epsl.2011.10.027>
- McQuarrie, N., Tobgay, T., Long, S. P., Reiners, P. W., & Cosca, M. A. (2014). Variable exhumation rates and variable displacement rates: Documenting recent slowing of Himalayan shortening in western Bhutan. *Earth and Planetary Science Letters*, 386, 161–174. <https://doi.org/10.1016/j.epsl.2013.10.045>
- Meert, J. G., & Pandit, M. K. (2015). Chapter 3 The Archaean and Proterozoic history of Peninsular India: tectonic framework for Precambrian sedimentary basins in India. *Geological Society, London, Memoirs*, 43(1), 29–54. <https://doi.org/10.1144/M43.3>
- Meert, J. G., Pandit, M. K., Pradhan, V. R., Banks, J., Sirianni, R., Stroud, M., Newstead, B., & Gifford, J. (2010). Precambrian crustal evolution of Peninsular India: A 3.0 billion year odyssey. *Journal of Asian Earth Sciences*, 39(6), 483–515. <https://doi.org/10.1016/j.jseas.2010.04.026>
- Mitra, S., Kainkaryam, S. M., Padhi, A., Rai, S. S., & Bhattacharya, S. N. (2011). The Himalayan foreland basin crust and upper mantle. *Physics of the Earth and Planetary Interiors*, 184(1–2), 34–40. <https://doi.org/10.1016/j.pepi.2010.10.009>
- Mohanty, S. (2012). Spatio-temporal evolution of the Satpura Mountain Belt of India: A comparison with the Capricorn Orogen of Western Australia and implication for evolution of the supercontinent Columbia. *Geoscience Frontiers*, 3(3), 241–267. <https://doi.org/10.1016/j.gsf.2011.10.005>
- Monsalve, G., Sheehan, A., Schulte-Pelkum, V., Rajaure, S., Pandey, M. R., & Wu, F. (2006). Seismicity and one-dimensional velocity structure of the Himalayan collision zone: Earthquakes in the crust and upper mantle. *Journal of Geophysical Research*, 111(B10), <https://doi.org/10.1029/2005JB004062>
- Mugnier, J. L., Leturmy, P., Mascle, G., Huyghe, P., Chalaron, E., Vidal, G., Husson, L., & Delcaillau, B. (1999). The Siwaliks of western Nepal: I. Geometry and kinematics. *Journal of Asian Earth Sciences*, 17(5), 629–642. [https://doi.org/10.1016/S1367-9120\(99\)00038-3](https://doi.org/10.1016/S1367-9120(99)00038-3)
- Mukhopadhyay, G., Mukhopadhyay, S. K., Roychowdhury, M., & Parui, P. K. (2010). Stratigraphic correlation between different Gondwana Basins of India. *Journal of the Geological Society of India*, 76(3), 251–266. <https://doi.org/10.1007/s12594-010-0097-6>
- Najman, Y., Burley, S. D., Copley, A., Kelly, M. J., Pander, K., & Mishra, P. (2018). The Late Eocene-Early Miocene unconformities of the NW Indian Intraplate basins and Himalayan foreland: A record of tectonics or mantle dynamics? *Tectonics*, 37(10), 3970–3985. <https://doi.org/10.1029/2018TC005286>
- Najman, Y., Carter, A., Oliver, G., & Garzanti, E. (2005). Provenance of Eocene foreland basin sediments, Nepal: Constraints to the timing and diachroneity of early Himalayan orogenesis. *Geology*, 33(4), 309–312. <https://doi.org/10.1130/G21161.1>
- Najman, Y., Jenks, D., Godin, L., Boudagher-Fadel, M., Millar, I., Garzanti, E., Horstwood, M., & Bracciali, L. (2017). The Tethyan Himalayan detrital record shows that India-Asia terminal collision occurred by 54 Ma in the Western Himalaya. *Earth and Planetary Science Letters*, 459, 301–310. <https://doi.org/10.1016/j.epsl.2016.11.036>
- Najman, Y., Johnson, K., White, N., & Oliver, G. (2004). Evolution of the Himalayan foreland basin, NW India. *Basin Research*, 16(1), 1–24. <https://doi.org/10.1111/j.1365-2117.2004.00223.x>
- Najman, Y. M. R., Pringle, M. S., Johnson, M. R. W., Robertson, A. H. F., & Wijbrans, J. R. (1997). Laser ⁴⁰Ar/³⁹Ar dating of single detrital muscovite grains from early foreland-basin sedimentary deposits in India: Implications for early Himalayan evolution. *Geology*, 25(6), 535–538. [https://doi.org/10.1130/0091-7613\(1997\)025<0535:LAADOS>2.3.CO;2](https://doi.org/10.1130/0091-7613(1997)025<0535:LAADOS>2.3.CO;2)
- Nakayama, K., & Ulak, P. D. (1999). Evolution of fluvial style in the Siwalik Group in the foothills of the Nepal Himalaya. *Sedimentary Geology*, 125(3), 205–224. [https://doi.org/10.1016/S0037-0738\(99\)00012-3](https://doi.org/10.1016/S0037-0738(99)00012-3)
- Negi, B. S., & Eremenko, N. A. (1968). *Tectonic map of India*. Oil and Natural Gas Commission.
- Nelson, K. D., Zhao, W., Brown, L. D., Kuo, J., Che, J., Liu, X., Klemperer, S. L., Makovsky, Y., Meissner, R., Mechie, J., Kind, R., Wenzel, F., Ni, J., Nabelek, J., Leshou, C., Tan, H., Wei, W., Jones, A. G., Booker, J., ... Edwards, M. (1996). Partially Molten Middle Crust Beneath Southern Tibet: Synthesis of project INDEPTH results. *Science*, 274(5293), 1684–1688. <https://doi.org/10.1126/science.274.5293.1684>
- Ojha, T. P., Butler, R. F., DeCelles, P. G., & Quade, J. (2009). Magnetic polarity stratigraphy of the Neogene foreland basin deposits of Nepal. *Basin Research*, 21(1), 61–90. <https://doi.org/10.1111/j.1365-2117.2008.00374.x>
- Ojha, T. P., Butler, R. F., Quade, J., DeCelles, P. G., Richards, D., & Upreti, B. N. (2000). Magnetic polarity stratigraphy of the Neogene Siwalik Group at Khutia Khola, far western Nepal. *Geological Society of America Bulletin, Geological Society of America*, 112, 424–434. [https://doi.org/10.1130/0016-7606\(2000\)112<424:MPSOT N>2.0.CO;2](https://doi.org/10.1130/0016-7606(2000)112<424:MPSOT N>2.0.CO;2)
- Parkash, B., Sharma, R. P., & Roy, A. K. (1980). The Siwalik group (Molasse) — Sediments shed by collision of continental plates. *Sedimentary Geology*, 25(1), 127–159. [https://doi.org/10.1016/0037-0738\(80\)90058-5](https://doi.org/10.1016/0037-0738(80)90058-5)
- Paul, H., Mitra, S., Bhattacharya, S. N., & Suresh, G. (2015). Active transverse faulting within underthrust Indian crust beneath the Sikkim Himalaya. *Geophysical Journal International*, 201(2), 1072–1083. <https://doi.org/10.1093/gji/ggv058>
- Pilgrim, G. E. (1913). The correlation of the Siwaliks with mammal horizons of Europe. *Records of the Geological Survey of India*, 42, 264–326.
- Prasad, B., & Asher, R. (2001). *Acritarch biostratigraphy and lithostratigraphic classification of Proterozoic and Lower Paleozoic sediments (Pre-unconformity sequence) of Ganga Basin, India*. Geoscience Research Group, Keshava Deva Malaviya Institute of Petroleum Exploration, Oil and Natural Gas Corporation.
- Quade, J., Cater, J. M., Ojha, T. P., Adam, J., & Harrison, T. M. (1995). Late Miocene environmental change in Nepal and the northern Indian subcontinent: Stable isotopic evidence from paleosols. *Geological Society of America Bulletin*, 107(12), 1381–1397. [https://doi.org/10.1130/0016-7606\(1995\)107<1381:LMECIN>2.3.CO;2](https://doi.org/10.1130/0016-7606(1995)107<1381:LMECIN>2.3.CO;2)
- Raiverman, V. (1983). Basin geometry, Cenozoic sedimentation and hydrocarbon prospects in north western Himalaya and Indo-Gangetic plains. *Petroleum Asia Journal, Petroliferous Basins of India*, 6(4), 67–92.
- Raiverman, V. (2002). *Foreland sedimentation in Himalayan tectonic regime: A relook at the orogenic process*. Bishen Singh Mahendra Pal Singh.
- Raiverman, V., Chugh, M. L., Srivastava, A. K., Prasad, D. N., & Das, S. K. (1994). Cenozoic tectonics of the fold belt of Himalaya and the Indo-Gangetic Fordeep with pointers towards hydrocarbon prospects. In S. K. Biswas, A. Dave, P. Garg, J. Pandey, A. Maithani, & N. J. Thomas (Eds.), *Proceedings of the second seminar on Petroliferous basins of India: Himalayan foothills, Vindhyan and Gondwana basins, geoscientific studies and hydrocarbon exploration techniques* (Vol. 3, pp. 25–54).

- Rao, M. R. (1973). The subsurface geology of the Indo-Gangetic plains. *Journal of the Geological Society of India*, 14(3), 217–242.
- Rao, N. P., Tiwari, V. M., Kumar, M. R., Hazarika, P., Saikia, D., Chadha, R. K., & Rao, Y. J. B. (2015). The Mw 6.9 Sikkim-Nepal earthquake of September 2011: A perspective for wrench faulting in the Himalayan thrust zone. *Natural Hazards*, 77(1), 355–366. <https://doi.org/10.1007/s11069-015-1588-y>
- Rasmussen, B., Bose, P. K., Sarkar, S., Banerjee, S., Fletcher, I. R., & McNaughton, N. J. (2002). 1.6 Ga U-Pb zircon age for the Chorhat Sandstone, lower Vindhyan, India: Possible implications for early evolution of animals. *Geology*, 30(2), 103–106.
- Ratschbacher, L., Frisch, W., Liu, G., & Chen, C. (1994). Distributed deformation in southern and western Tibet during and after the India-Asia collision. *Journal of Geophysical Research: Solid Earth*, 99(B10), 19917–19945. <https://doi.org/10.1029/94JB00932>
- Ravikant, V., Wu, F.-Y., & Ji, W.-Q. (2011). U-Pb age and Hf isotopic constraints of detrital zircons from the Himalayan foreland Subathu sub-basin on the Tertiary palaeogeography of the Himalaya. *Earth and Planetary Science Letters*, 304(3–4), 356–368. <https://doi.org/10.1016/j.epsl.2011.02.009>
- Ray, J. S. (2006). Age of the Vindhyan Supergroup: A review of recent findings. *Journal of Earth System Science*, 115(1), 149–160. <https://doi.org/10.1007/BF02703031>
- Ray, J. S., Martin, M. W., Veizer, J., & Bowring, S. A. (2002). U-Pb zircon dating and Sr isotope systematics of the Vindhyan Supergroup, India. *Geology*, 30(2), 131–134. [https://doi.org/10.1130/0091-7613\(2002\)030<0131:UPZDAS>2.0.CO;2](https://doi.org/10.1130/0091-7613(2002)030<0131:UPZDAS>2.0.CO;2)
- Regumi, A., Dhital, M., Gadtula, R., Tamrakar, N., & Yoshida, K. (2011). Lithostratigraphy and structures of the Siwaliks rocks in the southern part of Dang and its surrounding area, Southwestern Nepal. *Journal of the Faculty of Science Shinshu University*, 43, 1–42.
- Rösler, W., Metzler, W., & Appel, E. (1997). Neogene magnetic polarity stratigraphy of some fluviatile Siwalik sections, Nepal. *Geophysical Journal International*, 130(1), 89–111. <https://doi.org/10.1111/j.1365-246X.1997.tb00990.x>
- Sahni, M. R., & Mathur, L. P. (1964). *Stratigraphy of the Siwalik group* (Vol. 7). International Geological Congress.
- Sakai, H. (1983). Geology of the Tansen Group of the Lesser Himalaya in Nepal. *Memoirs of the Faculty of Science, Kyushu University, Series D Geology*, 25(1), 27–74. <https://doi.org/10.5109/1546083>
- Sakai, H. (1989). Rifting of the Gondwanaland and uplifting of the Himalayas recorded in Mesozoic and Tertiary fluvial sediments in the Nepal Himalayas. In A. Taira & F. Masuda (Eds.), *Sedimentary facies in the active plate margin* (pp. 723–732). Terra Scientific Publishing Company.
- Sakai, H., Hamamoto, R., & Arita, K. (1992). Radiometric ages of alkaline volcanic rocks from the upper Gondwana of the Lesser Himalayas, western Central Nepal and their tectonic significance: Kathmandu. *Bulletin of the Department of Geology, Tribhuvan University*, 2, 65–74.
- Sastri, V. V., Bhandari, L. L., Raju, A. T. R., & Datta, A. K. (1971). Tectonic framework and subsurface stratigraphy of the Ganga basin. *Journal of the Geological Society of India*, 12(3), 222–233.
- Searle, M. P., Law, R. D., Godin, L., Larson, K. P., Streule, M. J., Cottle, J. M., & Jessup, M. J. (2008). Defining the Himalayan main central thrust in Nepal. *Journal of the Geological Society*, 165(2), 523–534. <https://doi.org/10.1144/0016-76492007-081>
- Sengupta, S. N. (1962). Basement configuration of the Indo-Gangetic plains shown by aeromagnetic surveys. In *Proceedings of the seminar on oil prospects in the Ganga Valley* (Vol. 1, pp. 52–54). Oil and Natural Gas Corporation Technical Publications.
- Sharma, K. K., & Rahman, A. (2000). The Early Archaean-Paleoproterozoic crustal growth of the Bundelkhand craton, northern Indian shield. In M. Deb (Ed.), *Crustal evolution and Metallogeny in the Northwestern Indian shield: A Festschrift for Asoke Mookherjee* (pp. 51–72). Alpha Science International Ltd.
- Shukla, S. N., & Chakraborty, D. (1994). Status of exploration and future programme of hydrocarbon exploration in Vindhyan and Gondwana basins. In S. K. Biswas, A. Dave, P. Garg, J. Pandey, A. Maithani, & N. J. Thomas (Eds.), *Proceedings of the second seminar on Petroliferous basins of India: Himalayan foothills, Vindhyan and Gondwana basins, geoscientific studies and hydrocarbon exploration techniques* (Vol. 3, pp. 63–100). Indian Petroleum Publishers.
- Sitaula, R. P. (2009). *Petrofacies and Paleotectonic evolution of Gondwanan and Post-Gondwanan sequences of Nepal* (MSc thesis). Auburn University.
- Soucy La Roche, R., & Godin, L. (2019). Inherited cross-strike faults and Oligocene-early Miocene segmentation of the Main Himalayan Thrust, West Nepal. *Journal of Geophysical Research: Solid Earth*, 124(7), 7429–7444. <https://doi.org/10.1029/2019JB017467>
- Soucy La Roche, R., Godin, L., Cottle, J. M., & Kellett, D. A. (2018). Preservation of the early evolution of the Himalayan middle crust in Foreland Klippen: Insights from the Karnali Klippe, West Nepal. *Tectonics*, 37(5), 1161–1193. <https://doi.org/10.1002/2017TC004847>
- Srinivasan, S., & Khar, B. M. (1996). Status of hydrocarbon exploration in Northwest Himalaya and Foredeep – Contributions to stratigraphy and structure. In *Proceedings of the Symposium on NW Himalaya and Foredeep, Feb 1995* (Vol. 21, pp. 295–405). Geological Survey of India Special Publications.
- Stickroth, S. F., Carrapa, B., DeCelles, P. G., Gehrels, G. E., & Thomson, S. N. (2019). Tracking the growth of the Himalayan fold-and-thrust belt from lower Miocene foreland basin strata: Dumri formation. *Western Nepal. Tectonics*, 38(11), 3765–3793. <https://doi.org/10.1029/2018TC005390>
- Szulc, A. G., Najman, Y., Sinclair, H. D., Pringle, M., Bickle, M., Chapman, H., Garzanti, E., Andò, S., Huyghe, P., Mugnier, J.-L., Ojha, T., & DeCelles, P. (2006). Tectonic evolution of the Himalaya constrained by detrital 40Ar-39Ar, Sm-Nd and petrographic data from the Siwalik foreland basin succession, SW Nepal: Tectonic evolution of the Himalaya. *Basin Research*, 18(4), 375–391. <https://doi.org/10.1111/j.1365-2117.2006.00307.x>
- Turcotte, D. L., & Schubert, G. (2014). *Geodynamics* (3rd ed.). Cambridge University Press.
- Upreti, B. N. (1999). An overview of the stratigraphy and tectonics of the Nepal Himalaya. *Journal of Asian Earth Sciences*, 17(5–6), 577–606. [https://doi.org/10.1016/S1367-9120\(99\)00047-4](https://doi.org/10.1016/S1367-9120(99)00047-4)
- Valdiya, K. S. (1976). Himalayan transverse faults and folds and their parallelism with subsurface structures of north Indian plains. *Tectonophysics*, 32(3–4), 353–386. [https://doi.org/10.1016/0040-1951\(76\)90069-X](https://doi.org/10.1016/0040-1951(76)90069-X)
- Valdiya, K. S. (1980). *Geology of Kumaun Lesser Himalaya*. Wadia Institute of Himalayan Geology.
- van der Beek, P., Litty, C., Baudin, M., Mercier, J., Robert, X., & Hardwick, E. (2016). Contrasting tectonically driven exhumation and incision patterns, western versus central Nepal Himalaya. *Geology*, 44(4), 327–330. <https://doi.org/10.1130/G37579.1>
- Veevers, J. J., & Tewari, R. C. (1995). *Gondwana master basin of Peninsular India between Tethys and the interior of the Gondwanaland Province of Pangea* (Vol. 187). Geological Society of America Memoir. <https://doi.org/10.1130/0-8137-1187-8.1>
- Verma, A. K., Pati, P., & Sharma, V. (2017). Soft sediment deformation associated with the East Patna Fault south of the Ganga River,

- northern India: Influence of the Himalayan tectonics on the southern Ganga plain. *Journal of Asian Earth Sciences*, 143, 109–121. <https://doi.org/10.1016/j.jseaes.2017.04.016>
- Vögeli, N., Najman, Y., van der Beek, P., Huyghe, P., Wynn, P. M., Govin, G., van der Veen, I., & Sachse, D. (2017). Lateral variations in vegetation in the Himalaya since the Miocene and implications for climate evolution. *Earth and Planetary Science Letters*, 471, 1–9. <https://doi.org/10.1016/j.epsl.2017.04.037>
- White, N. M., Pringle, M., Garzanti, E., Bickle, M., Najman, Y., Chapman, H., & Friend, P. (2002). Constraints on the exhumation and erosion of the High Himalayan Slab, NW India, from foreland basin deposits. *Earth and Planetary Science Letters*, 195(1–2), 29–44. [https://doi.org/10.1016/S0012-821X\(01\)00565-9](https://doi.org/10.1016/S0012-821X(01)00565-9)
- Xiao, S., Tang, Q., Hughes, N. C., McKenzie, N. R., & Myrow, P. M. (2016). Biostratigraphic and detrital zircon age constraints on the basement of the Himalayan Foreland Basin: Implications for a Proterozoic link to the Lesser Himalaya and cratonic India. *Terra Nova*, 28(6), 419–426. <https://doi.org/10.1111/ter.12235>
- Yin, A. (2006). Cenozoic tectonic evolution of the Himalayan orogen as constrained by along-strike variation of structural geometry, exhumation history, and foreland sedimentation. *Earth-Science Reviews*, 76(1–2), 1–131. <https://doi.org/10.1016/j.earscirev.2005.05.004>
- Zhao, W., Nelson, K. D., Che, J., Quo, J., Lu, D., Wu, C., & Liu, X. (1993). Deep seismic reflection evidence for continental underthrusting beneath southern Tibet. *Nature*, 366(6455), 557–559. <https://doi.org/10.1038/366557a0>

SUPPORTING INFORMATION

Additional Supporting Information may be found online in the Supporting Information section.

How to cite this article: Duvall, M. J., Waldron, J. W. F., Godin, L., Najman, Y., & Copley, A. (2021). Indian plate structural inheritance in the Himalayan foreland basin, Nepal. *Basin Research*, 00, 1–25. <https://doi.org/10.1111/bre.12584>